

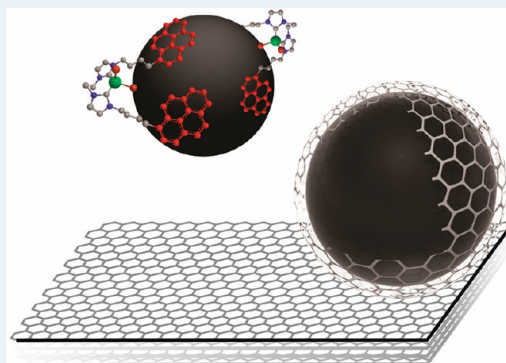
# Carbon Modifications and Surfaces for Catalytic Organic Transformations

Alexander Schaetz, Martin Zeltner, and Wendelin J. Stark\*

Institute for Chemical and Bioengineering, ETH Zürich, Wolfgang-Pauli-Strasse 10, 8093 Zürich, Switzerland

**ABSTRACT:** Carbon is anything but a new material, yet ubiquitously applicable for many catalytic transformations in modern organic chemistry. It is highly versatile, as it occurs as modifications abundantly available as 1–3D carbonaceous materials due to technical progress. In addition, materials such as activated charcoal, ordered mesoporous carbon (OMC), graphite and graphene (oxide), carbon nanotubes (CNTs), nanospheres (nanonions, fullerenes), and many others are no “innocent” supports, as demonstrated by many recent publications within the revitalized field of “carbocatalysis”. By nature, carbon scaffolds offer a perfect link between nanoscaled matter and organic molecules, which makes them an ideal cornerstone for molecular catalysts. Apart from this inherent chemical significance, the physical properties (e.g., different conductivity) are equally important for the performance of heterogeneous or immobilized homogeneous catalysts. Careful selection of the carbon scaffold enables control of reactivity by tuning the electronic interactions of active sites with the support or among each other. Moreover, separation and recycling of “heterogenized” catalysts can be further improved by rendering carbon “magnetic”, that is, by incorporation of magnetic particles or by coating metal nanomagnets with graphene-like shells. Altogether, tuning the properties of carbon supports might lead to catalysts tailored not only in matters of reactivity (electron shuttle), but also to down-to-earth problems such as purification (magnetic separation and recycling). This critical review will highlight how far such concepts have already been implemented in the design of “heterogenized” catalysts and is meant to widen the perspectives where certain concepts have yet to be realized.

**KEYWORDS:** graphene, carbon onions, carbon nanotubes, carbon-coated, support, carbocatalysis



## INTRODUCTION AND SCOPE

The main purpose of carbon as a support material was originally believed to be limited to enabling and maintaining a well-dispersed form of a metal catalyst, that is, by keeping the metal crystallites separated from each other so they would not form agglomerates or sinter into larger clusters upon heating. This concept of a more or less “innocent” support had to be replaced by one that accounts for the various interactions between metal particles and the solid matrix via surface functionalities (e.g., acidic groups) and the electronic character of the support itself. The evaluation of the extent of these “metal–support interactions” and rationalizations or even predictions regarding their influence on the activity of catalytic species might be the most interesting challenge for the design of novel heterogeneous catalysts.

These interactions depend strongly on the nature of the metal, but also on the chosen carbon support, since the chemical and physical properties of any given carbon strongly depends on its source and preparation method.

Natural sources for carbons may be divided into two classes: well-defined ones with uniform hybridization and long-range order (e.g., graphite) and ill-defined ones, such as glassy or amorphous carbons.<sup>1,2</sup> Synthetic carbons such as charcoal (recovered after pyrolysis of organic compounds) and activated carbons (chemically treated porous carbons with enhanced

adsorptive properties)<sup>3</sup> are members of the latter division. Examples of well-defined carbons include naturally occurring allotropes, such as fullerenes and graphene, as well as carbon nanotubes and spheres with a high graphitic fraction. The layout of this review article is orientated along the carbon modifications relevant as catalyst supports; namely, amorphous carbon, graphite, graphene/graphene oxide, carbon nanotubes, and C<sub>60</sub> (Figure 1).

With modern synthetic supports that enter the nanoregime, it becomes more and more difficult to physically separate the heterogeneous matrixes after use, a price one pays for the high dispersion stability and reduced mass transfer limitations when using nanosized materials. Therefore, an alternative separation method will be introduced, that is, rendering carbon scaffolds “magnetic”. Each chapter will start with a brief description of the carbon support, with a strong focus on its physical and chemical properties. The following subsection is dedicated to carbocatalysis,<sup>4–6</sup> the use of (presumably) metal-free, heterogeneous carbons as catalysts in synthetic reactions. It will illustrate that carbon is by no means an inert support and that careful choice of the support is vital for catalytic applications.

**Received:** January 9, 2012

**Revised:** March 12, 2012

**Published:** April 27, 2012

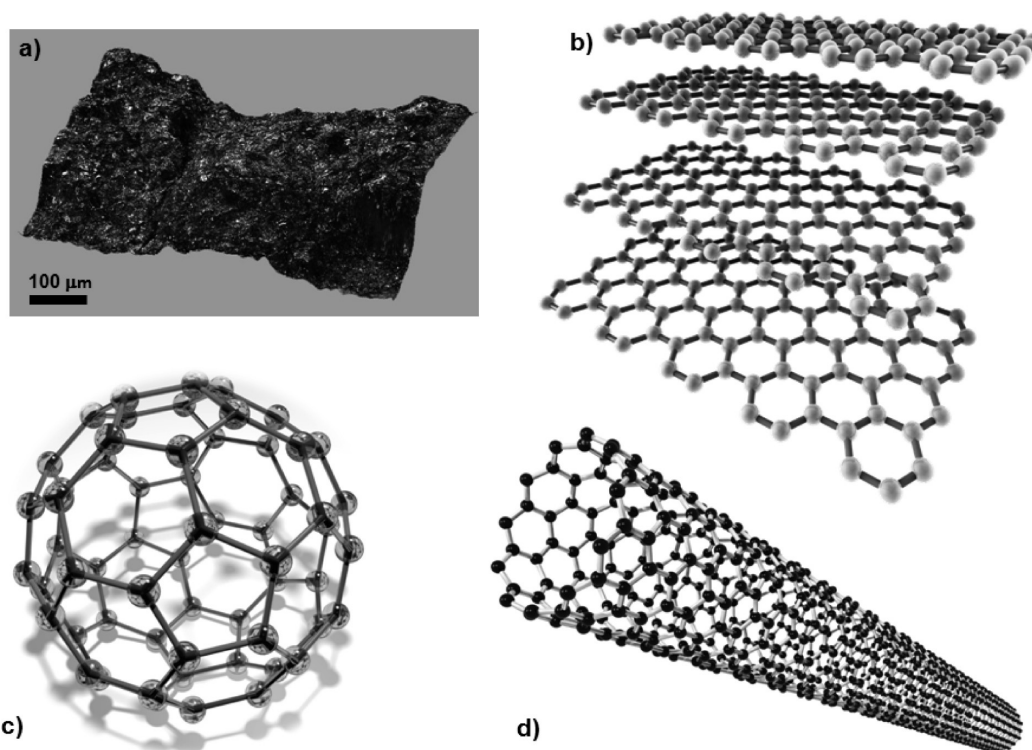


**Figure 1.** Representation of relevant carbon allotropes in catalysis: (a) activated carbon (Norit), (b) graphite, (c) Buckminster fullerene ( $C_{60}$ ), (d) carbon nanotube.

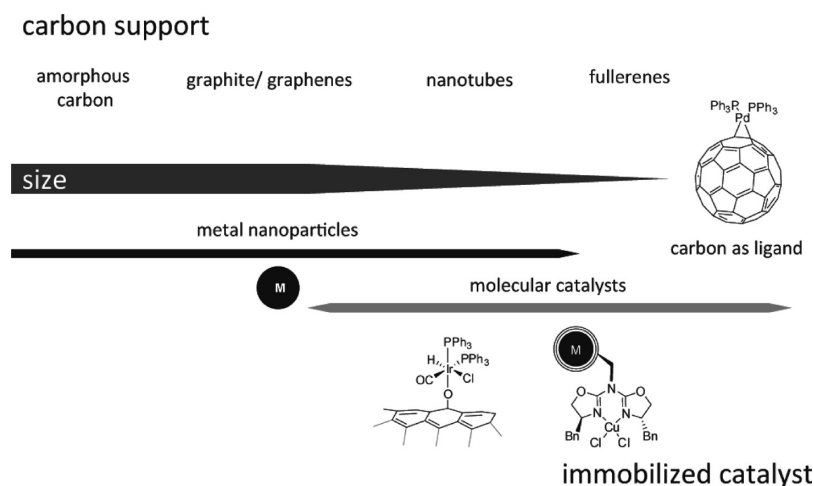


**Figure 2.** Outline of the supports discussed as a function of size. Catalytically active species consist of metal nanoparticles (common with all allotropes), molecular catalysts (uncommon only with amorphous carbon), and metal–carbon complexes (common only with fullerenes).

Subsequently, the role of carbon as a support for metal (oxide) nanoparticles and molecular catalysts (covalently and non-covalently immobilized metal complexes and organocatalysts) will be discussed (Figure 2).

In view of the large body of publications in this exciting field, the examples shown are not meant to be exhaustive but merely representatives of the subjects. Since this work may be considered a critical review, additional emphasis will be put on the discussion of drawbacks and future perspectives.

## 1. AMORPHOUS CARBON: ACTIVATED CHARCOAL

Carbon materials differ in their structure, which results in the variation of surface free energy characteristics and ultimately in

altered adsorption profiles. Distinctions can be made by inverse gas chromatography, indicating the presence of at least three types of adsorption sites in amorphous carbon:<sup>7</sup> they consist of centers of weak, strong, and very strong (irreversible) adsorption. The weak adsorption area is believed to consist mainly of basal planes of graphene-like carbon; the strong adsorption centers, of aggregates and graphene fragments. The irreversible adsorption centers are located in micropores. In contrast to amorphous carbon, most carbon allotropes have a strong prevalence for only one or two different adsorption sites. For example, fullerene-like carbons possess only weak adsorption areas.

Inexpensive activated carbons (charcoal) are widely used as solid supports for metal catalysts,<sup>8,9</sup> since they are stable under

acidic and basic conditions, have a much higher surface area than alumina or silica ( $>1000 \text{ m}^2 \text{ g}^{-1}$ ),<sup>10</sup> and feature superior attrition resistance. In addition, the flammability of activated carbons may be considered an advantage, because it means easy refining and recycling. Having these attractive features in mind, it is hard to imagine how charcoal could not become a much more abundant matrix for commercial catalytic applications, mostly as a support for metallic nanoparticles.

**1.1. Carbocatalysis.** Most of the reactions involving activated charcoals as carbocatalysts are oxidations using atmospheric oxygen or hydrogen peroxide as the terminal oxidants. In the 1930s, it was discovered that activated charcoals are capable of catalyzing the aerobic oxidation of ferrocyanide ( $\text{Fe}(\text{CN})_6^{4-}$ ) to ferricyanide ( $\text{Fe}(\text{CN})_6^{3-}$ ).<sup>11,12</sup> It was reasoned that thermal activation of the carbon surface generated acidic sites that facilitated the adsorption of oxygen. A similar mechanism was made responsible for the activated charcoal catalyzed oxidation of oxalic acid via the generation of surface-bound geminal diols.<sup>13–15</sup> Akin to processes that take place on inorganic oxides,<sup>16</sup> Lewis acid catalysis might take place on acidic carbon surfaces, as well. A recent exception to the predominant oxidation reactions is the reduction of fatty acids (e.g., palmitic acid) in the presence of activated carbon in (near-) supercritical water ( $T_C = 374 \text{ }^\circ\text{C}$ ).<sup>17</sup> Next to decarboxylation of the acid moiety, the internal unsaturated moiety was reduced to afford pentadecane (33% conversion); however, the nature of the terminal reductant remains unclear.<sup>18</sup>

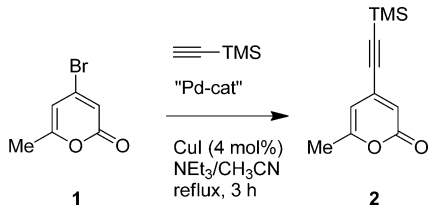
**1.2. Metal Clusters on Activated Carbon.** Carbon-supported metals are complex in nature, and their preparation, albeit not very difficult, is crucial for the performance of the final catalyst. Different conditions can alter the interplay of activity, selectivity, and catalyst leaching/lifetime. Methods such as wet or dry impregnation, deposition–precipitation, deposition–reduction, or ion-exchange protocols are routinely applied. Most of them rely on the treatment with aqueous solutions of suitable precursors, such as metal salts.<sup>19</sup> Transition metal clusters (e.g., palladium) immobilized on charcoal are quite common in modern chemistry, especially as hydrogenation catalysts. It would be far beyond the scope of this review to discuss their numerous synthetic applications. In addition, the mechanistic of hydrogenation are well understood and the subject of many excellent articles to which the interested reader may be referred.<sup>20–25</sup>

“Pd/C” as a shortcut is somewhat misleading because it suggests a uniformity that is foreign to the natural product charcoal. The Pd (1–20 wt %) and water (up to 50 wt %) contents, as well as the level of surface oxidation, varies with the batch quality and supplier, which makes a direct comparison between different studies complicated. The palladium distribution pattern is another critical parameter.<sup>26,27</sup> This is especially true for cross-coupling reactions, another important field of application for heterogeneous palladium catalysts. However, considerable effort was dedicated to the quality control of Pd/C by industry in past decades. Because of the enormous relevance of C–C bond formations associated with names such as Heck, Stille, Suzuki, Sonogashira, and Negishi, several reviews have highlighted the use of Pd/C catalysts in these reactions over past years;<sup>28–31</sup> however, the mechanisms (heterogeneous vs homogeneous) of Pd/C-catalyzed coupling reactions are not yet fully understood and are the source of some controversy.

*The Active Species: Heterogeneous or Homogeneous?* Some reports are quite intriguing, especially when homoge-

neous and heterogeneous systems result in different yields or regioselectivity. An interesting case is the Sonogashira coupling of 2-pyrone **1**, which proved quite unsuccessful under homogeneous conditions in a variety of solvents. The best results were obtained with a Pd/C-based catalyst (Table 1, entry 5).<sup>32</sup>

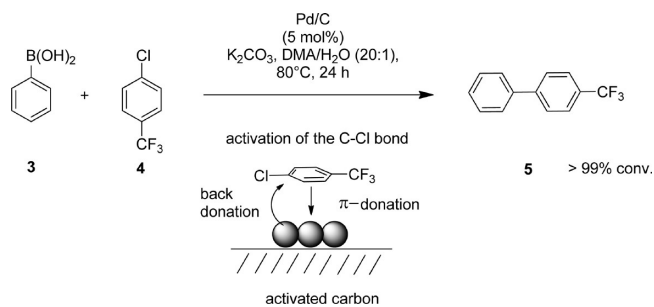
**Table 1. Sonogashira Coupling of 2-Pyrone, **1**, with Trimethylsilyl (TMS) Acetylene Catalyzed by Different Homogeneous and a Heterogeneous Palladium Source**



entry	palladium source	PPh <sub>3</sub> (mol %)	conv (%)
1	Pd(PPh <sub>3</sub> ) <sub>2</sub> Cl <sub>2</sub> (6 mol %)	–	–
2	Pd(OAc) <sub>2</sub> (6 mol %)	18	50
3	Pd(PPh <sub>3</sub> ) <sub>4</sub> (6 mol %)	–	47
4	Pd <sub>2</sub> dba <sub>3</sub> ·CHCl <sub>3</sub> (2.5 mol %)	15	69
5	Pd/C (20 mol %)	25	82

A similar rise in the catalytic activity of some Pd/C-based systems with electron-poor arylchlorides (e.g., in Suzuki-coupling reactions) was rationalized with “synergistic anchimeric and electronic effects”.<sup>33</sup> Aryl chlorides are known to adsorb on Pd(111) surfaces, mainly via  $\pi$ -electrons, resulting in a nearly parallel orientation of the aromatic moiety (Scheme 1).

**Scheme 1. Pd/C-Catalyzed Suzuki Cross-Coupling with Electron-Poor Aryl Chloride **4****



This leads to an increased electron density on the Pd surface ( $\pi$ -donation) and facilitates the interaction (back-donation) of a separate but nearby Pd site with the C–Cl bond (anchimeric effect). Moreover, the  $\pi$ -donation reduces the electron density of the aryl ring, which further weakens the C–Cl bond (electronic effect). These cooperative anchimeric and electronic effects are absent in single-site homogeneous catalysts, which might account for the enhanced reactivity of Pd/C catalysts. Indeed, the heterogeneous system performed way better in Suzuki couplings with arylchlorides than homogeneous counterparts, such as palladium acetate and palladium(II) bis(ethylthio)dichloride [ $\text{PdCl}_2(\text{SET})_2$ ].<sup>34</sup>

Such interactions of a substrate with clusters of Pd atoms would be a truly heterogeneous pathway, as it is known for hydrogenation reactions using transition metal catalysts (chemisorption of hydrogen on a metal surface).<sup>35–39</sup>

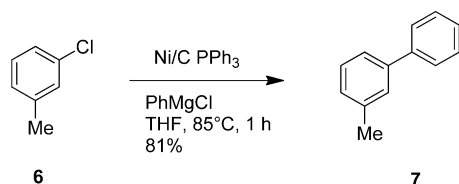


Furthermore, the use of phosphine ligands proved to be dispensable in some Pd/C-catalyzed C–C bond formations.<sup>40</sup>

However, an exclusively heterogeneous mode of action is by far not the only mechanism that accounts for immobilized metal clusters. Indeed, many authors tend to claim that the contribution of the heterogeneous catalyst is rather insignificant and that it acts merely as a reservoir for dissolved metal species, which may be considered the active catalyst form. For example, Arai et al. clearly observed, in accordance with previous investigations, a prevailing homogeneous course in Heck reactions, although heterogeneous catalysts were applied.<sup>41,42</sup> Hence, they claimed that mainly the dissolved Pd species ( $\text{Pd}_{\text{sol}}$ ) is active because the reaction rates increased with the amount of leached palladium. Similar trends for charcoal-supported Pd catalysts were reported for the Sonogashira reaction,<sup>29</sup> carbonylation of allyl ethers,<sup>43</sup> or the allylation of aniline with allylacetate.<sup>44</sup>

It is far beyond the scope of this work to discuss whether a heterogeneous or a homogeneous pathway prevails for a catalyst under certain conditions. Neither shall the various influences on the leaching behavior of charcoal-supported transition metal catalysts be discussed, which depend on preparation methods (e.g., impregnation, washing, drying) as well as reaction conditions (concentration of ligands, reaction temperature, solvent), among many others. Nevertheless, even when thinking of a solid matrix only as a carrier and with the catalytic cycle maintained by metal species bleeding into solution, this does not mean that the nature of the support is rendered insignificant. Desorption and, more interestingly, reabsorption is highly dependent on the nature of the support. It was found that redeposition of palladium species occurs more rapidly on carbon than on other supports, for example, zeolites.<sup>41</sup> Although a maximum of 55% of the immobilized Pd was detected in solution during the course of a Heck reaction, it was nearly completely reabsorbed on the charcoal support after consumption of aryl iodide. Such time-dependent profiles were occasionally reported for Pd/C catalysts,<sup>45,46</sup> which clearly shows that it is not always valid to judge the influence of dissolved metal species by the final concentration in the reaction media. Doing so might have led to conclusions that should be reconsidered in the light of these results; however, such a bleeding behavior is, of course, not typical for every transition metal catalyst. In the case of Ni/C, the amount of detectable  $\text{Ni}_{\text{sol}}$  was essentially constant and extremely low at any stage of a Kumada coupling reaction (Scheme 2).<sup>47</sup>

**Scheme 2.** Ni/C-Catalyzed Kumada Coupling of an Arylchloride **6** with a Phenyl-Grignard Reagent

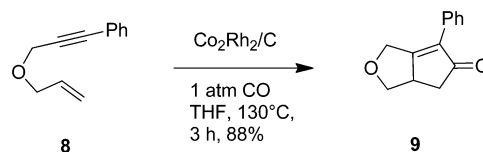


Many recent publications place emphasis on the role of leached metal species. Without going into detail, it should be noted that acquiring such data can once again create misleading results, for example, when a catalyst is filtered off during an ongoing reaction (cold or hot) and the filtrate is re-exposed to the reaction conditions: during the filtration process, substrates or reagents may be redeposited on the charcoal. Hence, failure

of a filtered reaction mixture to furnish further product does not guarantee that dissolved species are devoid of any activity. Reactions with polymer-bound ligands (“three-phase tests”) might give more reliable information on the origin of the active species.<sup>48–50</sup>

Another elegant test that gives some evidence for distinguishing between homogeneous and heterogeneous catalysis is the so-called mercury-poisoning experiment. The poisoning through  $\text{Hg}(0)$  by amalgamating a heterogeneous metal(0) catalyst<sup>51</sup> or adsorbing onto its surface made it a most widely used test.<sup>52,53</sup> In addition, in here, the results have to be interpreted carefully, since  $\text{Hg}(0)$  reacts with some metal complexes. Consequently, the suppression of catalysis is not always evidence for a heterogeneous pathway, but no poisoning by  $\text{Hg}(0)$  marks reliably a homogeneous mode of action. Such an experiment was conducted with Co/Rh heterobimetallic nanoparticles immobilized on charcoal, which lost their ability to catalyze intra- and intermolecular Pauson–Khand-type reactions upon addition of mercury (Scheme 3).<sup>54</sup>

**Scheme 3.** Example of a  $\text{Co}_2\text{Rh}_2/\text{C}$ -Catalyzed Intramolecular Pauson–Khand Type Reaction



The situation might be even more complicated, since the main fraction of dissolved species is probably trapped within the charcoal matrix, either mechanically or via a plethora of possible interactions (e.g., van der Waals attractions, Coulomb interactions, ion exchange interactions with metal nuclei). This might include the formation of  $\pi$ -complexes in which graphene acts as a ligand, especially in lamellar compounds of graphite (LCG).<sup>55</sup> The most interesting question in this regard might be, How far do the dissolved species in the pores take part in the catalytic reaction? This and many other questions have yet to be answered. Despite these mechanistic implications and the ongoing discussion whether the active catalyst species is actually heterogeneous, charcoal is maybe the most prominent example for a carbon support, simply because it is so inexpensive.

**1.3. Molecular Catalysts on Activated Carbon.** Organometallic complexes on activated carbons are comparatively rare. Especially adsorption of molecular catalysts on activated carbons is, in general, less efficient, because the oxygenated surface hampers  $\pi$ -stacking interactions between the support and aromatic moieties in the catalyst. A recent study using different commercial charcoals indicated a clear correlation between increasing surface oxygen content of the supports and decreasing adsorption of a naphthoic acid-anchored rhodium catalyst **10** (Figure 3).<sup>56</sup> All of the carbons exhibited Brunauer–Emmett–Teller surface areas between 960 and 1900  $\text{m}^2 \text{g}^{-1}$ , indicative for a high microporous volume into which the catalyst was nevertheless adsorbed to a significant extent (>1 wt % Rh). Adsorption proved to be mainly irreversible in these pores, and it was never demonstrated that this catalyst is actually active.

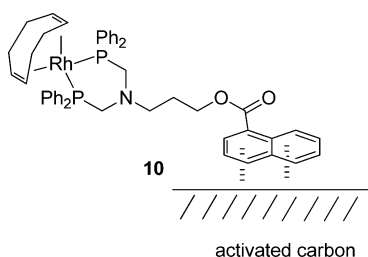


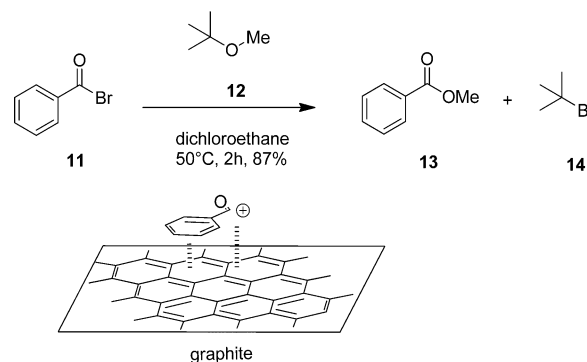
**Figure 3.** A molecular rhodium catalyst immobilized on activated charcoal via  $\pi$ -stacking interactions.

## 2. GRAPHITE, GRAPHENE AND CHEMICALLY MODIFIED GRAPHENES

Graphene and other two-dimensional  $sp^2$ -hybridized carbon scaffolds had a tremendous impact in the area of catalysis, mainly because of their unique electrical properties, especially in comparison with other carbon materials.<sup>57</sup> Although graphene was known to exist within graphite materials, it was assumed to be thermodynamically unstable in distinct 2D structures at finite temperatures.<sup>58</sup> In 2004, this hypothesis was disproved by the experimental discovery of graphene.<sup>59</sup> Geim et al. mechanically exfoliated single sheets from the  $\pi$ -stack layers in graphite for the first time, which demanded not less than 5.9 kJ mol<sup>-1</sup> carbon because of cohesive van der Waals forces.<sup>60</sup> The unique electron transfer properties of graphene, such as a half-integer quantum Hall effect, the massless Dirac fermion behavior of its charge carriers, and quantum capacitance, have been extensively discussed in several reviews.<sup>61–66</sup> Graphene features both semiconducting and metallic characteristics; hence, it can be either considered a metal with vanishing Fermi surface or a semiconductor with a vanishing band gap.<sup>67</sup> Its electron mobility is remarkably high (>1000 cm<sup>2</sup> V<sup>-1</sup> s<sup>-1</sup>) and nearly temperature-independent between 10 and 100 K.<sup>65</sup> Although the use of graphene-based nanomaterials as catalyst support has been hampered by the high price associated with the laborious synthesis and processing (e.g., sublimation of silicon from silicon carbide wafers,<sup>68</sup> chemical vapor deposition,<sup>69</sup> oxidation/reduction protocols<sup>70</sup>), significant advances have been achieved in the recent years and may break ground for future applications.<sup>71,72</sup>

**2.1. Carbocatalysis.** Many of the early studies concerning carbocatalysis with graphitic compounds focused on simple redox processes, but the field has progressed to demonstrate that carbons can facilitate more sophisticated reactions, including complex functional group transformations and carbon–carbon or carbon–heteroatom bond formations. For example, graphite has been found to catalyze the cleavage of alkyl or aromatic ethers (**12**) using acyl halides, such as **11**, to yield the corresponding esters (**13**) in good to excellent yields (Scheme 4).<sup>73</sup> Primary and secondary alkyl ethers did not react under these conditions, which is indicative for a  $S_N1$  type reaction. However, the authors proposed that cationic intermediates such as the acylium cation are stabilized due to  $\pi$ -interactions akin to a Lewis acid type mechanism (Scheme 4). In general, this hypothesis is supported by a similar effect of graphite in Friedel–Crafts type substitutions between various benzylhalides and electron-rich aromats, which furnished different diphenyl methanes in 38–99% yield.<sup>74</sup> Such electronic effects of carbon surfaces might render the catalytic activity of immobilized metal clusters or complexes; hence, it is highly important to validate and fully understand these interactions.

### Scheme 4. Graphite Catalyzed Cleavage of Alkyl Ether **12** with Acyl Chloride **11** To Yield Ester **13**



To this end, carbocatalysis is an important tool if the influence of trace metals is excluded meticulously and the physical contribution of the carbon surface can be studied in its purest form.

Another physical property of graphite is its significantly high thermal conductivity (19 W cm<sup>-1</sup> K<sup>-1</sup> at 300 K);<sup>75</sup> thus, it has been used as a solid state thermal conductor. After physisorption on graphite, anthracene (**15**) was susceptible to [4 + 2] cycloaddition reactions with several electron-deficient dienophiles (e.g., dimethyl but-2-ynedioate) when the system was exposed to microwave irradiation (Scheme 5).<sup>76,77</sup> Conventional heating in refluxing xylene demanded considerably longer reaction times (hours rather than minutes).

Although mostly activated (i.e., oxidized) carbons are commonly used as catalysts for oxidation reactions (see section 1.1), reduced forms such as graphite account mainly for reductions. With hydrazine hydrate as the terminal reductant, graphite catalyzes the reduction of nitroarenes to the corresponding anilines (up to 98% conversion).<sup>78</sup> Substrate adsorption, which should facilitate electron transfer from hydrazine, was claimed as a key step; however, also aliphatic species with a presumably weaker interaction to the surface could be transformed at similar rates. With either graphite or hydrazine absent, no reaction was observed.

Oxidized forms of graphitic materials, such as graphite oxide and graphene oxide (GO), which are common precursors for graphene-like materials, are maybe the most abundant carbon scaffolds for oxidation reactions.<sup>79,80</sup> Graphite (and graphene) oxide can be prepared by the Hummers reaction, which was first reported in 1958.<sup>81</sup> Briefly, graphite is treated with potassium permanganate and sodium nitrate in concentrated sulfuric acid. The reaction is subsequently quenched with aqueous hydrogen peroxide, which delivers a product with increased hydrophilicity. Water readily intercalates into GO, which is responsible for the significantly altered stacking structure, for example, interlamellar *d* spacings stretched from 3.5 Å to a maximum of 8.0 Å.<sup>82,83</sup> A widely accepted structural representation of this material contains mainly epoxides and alcohols within the plain and predominantly carboxylic acids at the edges and defects (Figure 4).<sup>84–86</sup>

Graphite oxide and GO were shown to significantly facilitate the oxidation of a variety of alcohols to the corresponding carbonyl compounds (Table 2). No conversion was observed when graphite oxide was used without terminal oxidant (i.e., under nitrogen atmosphere) or with hydrazine-reduced GO and natural flake graphite, respectively.<sup>5</sup> Interestingly, the stereochemistry of the substrates was also discriminated to

Scheme 5. Microwave-Assisted [4 + 2] Cycloaddition Reaction between Dimethyl but-2-ynedioate and Anthracene 15, Facilitated by Physisorption of 15 on Graphite and Its Thermal Conductivity

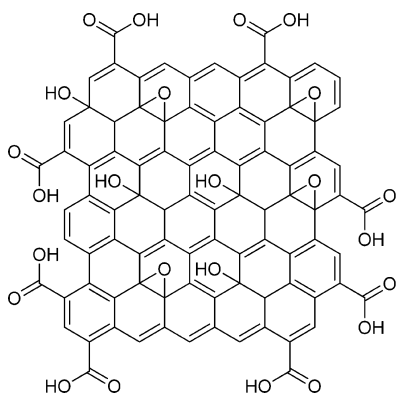
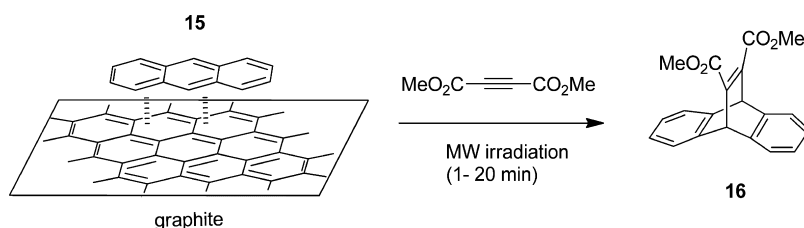


Figure 4. Proposed structure of graphene oxide according to Lerf et al.<sup>50</sup>

some extent: *cis*-stilbenes underwent a Wacker-type oxidation (Table 2, entry 4) whereas *trans*-stilbenes proved basically unreactive.<sup>5</sup> Sometimes, the role exerted by graphite oxide is not completely catalytic in nature. The hydration of alkynes **25**, **27**, and **29** (entries 5–7), which proceeded at rather low temperatures (<100 °C), rendered the oxygen content of graphite oxide significantly lower. This might be due to thermal degradation or consumption of surface-bound oxygen by the alkynes.

Graphite oxide is acidic in aqueous media (pH 4.5 at 0.1 mg mL<sup>-1</sup>),<sup>87</sup> an attribute which enabled a tandem reaction, as shown in an elegant study by Bielawski et al. They started with the aforementioned oxidation of benzylic alcohol **31** and phenylacetylene derivative **32** in a one-pot reaction, which gave rise to a subsequent acid-catalyzed Claisen–Schmidt condensation of the carbonyl compounds (entry 8).<sup>88</sup>

**2.2. Metal Clusters on Graphitic Carbon.** A major application field for graphitic carbons is the immobilization of metal nanoparticles, which comes naturally and with similar issues, as discussed in a previous chapter (1.2). In lieu of many excellent studies, the work of Muelhaupt et al. will be quoted, demonstrating remarkable turnover frequencies (TOF > 39 000 h<sup>-1</sup>) in Suzuki–Miyaura cross-coupling reactions using palladium nanoparticles dispersed on graphite oxide.<sup>89</sup> These results may be closely associated with the impressive theoretical surface values of exfoliated (oxidized) graphene sheets (2600 m<sup>2</sup> g<sup>-1</sup>).<sup>90</sup> Such values are hard to achieve with graphene itself because of the strong van der Waals interactions among the individual sheets, thus resulting in aggregation. However, to harness the redox properties of this two-dimensional catalyst support, the use of reduced graphene oxide (rGO) is much more suggestive. In any case, it is highly important to ensure and maintain an excellent dispersion of the catalytic metal sites during the preparation of the supported catalyst system. In this regard, a very successful method was reported by Gupton et al.,

Table 2. Reactions over Graphite Oxide<sup>a</sup>

entry	starting material	product	conv. <sup>[b]</sup> (%)
1			> 98
2			> 98
3			> 98
4			56
5			> 98
6			52
7			27
8			61 <sup>[c]</sup>

<sup>a</sup>Graphite oxide (5–200 wt %), 25–100 °C, 3–144 h, solvent-free.

<sup>b</sup>Determined by <sup>1</sup>H NMR. <sup>c</sup>Isolated yield.

who introduced a microwave-assisted chemical reduction of well-dispersed GO and palladium salt to form Pd/rGO.<sup>91,92</sup> This material demonstrated outstanding catalytic activity for the Suzuki–Miyaura coupling reaction (TOF up to 108 000 h<sup>-1</sup>) under ligand-free conditions using microwave irradiation, which was attributed to the high concentration of well dispersed Pd-NPs. An alternative approach is based on pulsed laser (532 nm) irradiation of a GO dispersion in the presence of a Pd(II) source. The partially reduced GO thus obtained offers a multitude of defect sites tagged with Pd clusters. Excellent turnover numbers (TON) of 7800 and frequencies (230 000 h<sup>-1</sup>) were observed in the Suzuki–reaction under microwave irradiation.<sup>92</sup> The scope of this method could be

further extended for the synthesis of Pt, CoO, and Pd–CoO alloy nanoparticles immobilized on partially reduced GO.<sup>93</sup>

**2.2.1. Electrocatalysis.** Heterogeneous electrocatalysis is focused on reactions occurring in an electrochemical cell at the electrode surface.<sup>93</sup> Graphite and graphene, as well as their derivatives, are excellent and widespread carbon mediators in such redox systems,<sup>94</sup> although other allotropes have also been applied (e.g., C<sub>60</sub>,<sup>95</sup> carbon nanotubes,<sup>96</sup> boron-doped diamond<sup>97</sup>). Although carbon-based scaffolds usually act as a support for catalytic metal centers, metal-free “carbon alloys”,<sup>98</sup> such as boron- and nitrogen-doped carbons (N-carbon) were reported as promising promoters for the oxygen reduction reaction (ORR) within proton exchange membrane fuel cells.<sup>99</sup> The activity of these systems ranges between nonmodified carbons and their metal doped analogs.

For applications in electrocatalysis, it is advantageous to maintain a well-ordered structure of the carbon matrix; hence, post-treatment of carbonaceous materials (e.g., with ammonia at 600–900 °C) is preferred over in situ synthesis of N-doped carbons. Sidik et al.<sup>100</sup> reported on such a material for the ORR, but the nature of the active sites remains a source of some controversies. The enhanced activity of the “carbon alloys” was attributed to the presence of pyridinic nitrogens, the increased number of edge plane defects caused by the propensity of incorporated nitrogen to form pentagonal defects in the graphene stacking (“turbostratic disorder”), or the increased stability of the strongly Lewis basic carbons toward oxidation.<sup>99</sup> Albeit the catalytic activity of N-doped carbons is still low in the ORR compared to Pt-doped carbons, nitrogen is an indispensable element in many carbon-supported metal catalysts (e.g., Fe or Co) with potential applications in fuel cells. However, among all metal nanoparticle-based electrocatalysts, platinum dispersed on carbon is the most abundant in fuel cells. For example, proton-exchange membranes were assembled using Pt/rGO as cathode material, and Pt dispersed on carbon black, as the anode.<sup>101</sup> In comparison with a hydrogen fuel cell featuring an unsupported Pt cathode, a different voltage decay profile was observed. The partially discharged Pt/rGO-based fuel cell delivered up to 161 mW cm<sup>-2</sup>, significantly more than the unsupported analog (96 mW cm<sup>-2</sup>).

In the field of electrocatalysis, it is especially challenging to correlate the catalyst efficiency with the various parameters, which may be illustrated by a recent topic. The performance of rechargeable lithium batteries is currently limited by charge/discharge cycling and the quantity of lithium that can be removed from and reinserted into the positive intercalation electrode (Li<sub>x</sub>CoO<sub>2</sub>, 0.5 < x < 1). The negative electrode consists of graphite, which hosts lithium between its graphene layers in the charged state. Substituting the negative intercalation electrode with a porous electrode (Figure 5), thus allowing Li to react directly with ambient oxygen, would increase the theoretical charge storage by 1 order of magnitude.<sup>102</sup> A prerequisite for such a setup is the efficient decomposition of Li<sub>2</sub>O<sub>2</sub> (oxygen evolution reaction) to recharge the battery, which may be accelerated by an electrocatalyst, that is, metal (platinum and gold supported on carbon) or metal oxide ( $\alpha$ -MnO<sub>2</sub> nanowires in carbon).<sup>102–104</sup> Otherwise, large overpotentials would result in energy storage inefficiency (much more energy is needed to charge the battery than is released during discharge).

In a recent study on the efficacy of electrocatalysts in nonaqueous Li/O<sub>2</sub> batteries, Luntz et al. showed that the role

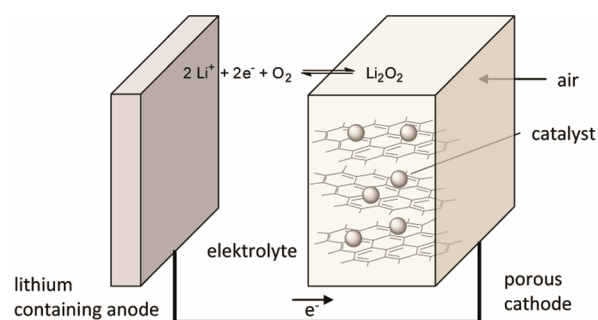
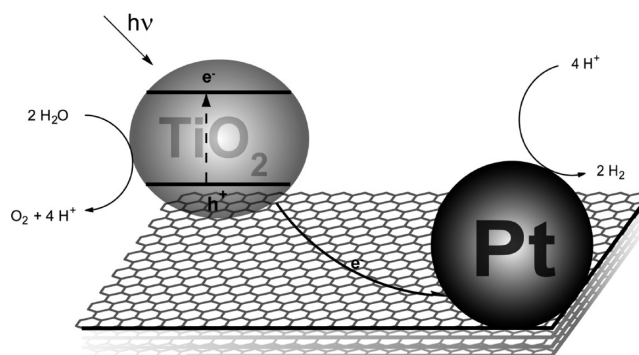


**Figure 5.** Schematic representation of a rechargeable Li/O<sub>2</sub> battery that relies on the electrocatalytic decomposition of lithium (per)oxide.

exerted by some of the currently used metal or metal oxide nanoparticles in the oxygen evolution is negligible.<sup>105</sup> Indeed, true electrocatalysis would demand a sufficiently mobile reactant and product in the rate-limiting step. Since neither Li<sub>2</sub>O nor Li<sub>2</sub>O<sub>2</sub> is soluble in nonaqueous electrolytes, surface diffusion, as expected for crystalline Li<sub>2</sub>O<sub>2</sub>, is the only way of ensuring such mobility around the active sites. However, the authors found that this diffusion is apparently not fast enough for effective catalysis, since the potential at which oxygen was initially evolved from low depth-of-discharge cells (~2.9 V) was only slightly above the open circuit potential of a discharged cell (~2.8 V). Earlier studies did not correlate coulometry (e.g., constant current discharge/charge cycles) with gas consumption/evolution data; hence, they observed decomposition (CO<sub>2</sub> evolution) of the solvent, which was actually the catalyzed reaction.

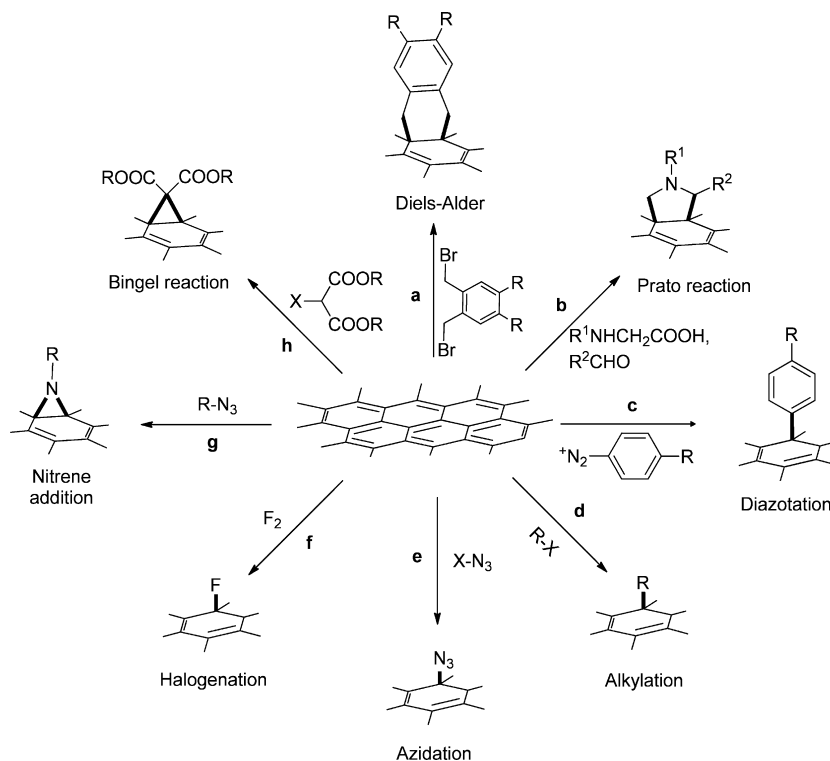
**2.2.2. Photocatalysis.** Incorporating two or more different types of particles in graphene or reduced graphene oxide sheets is a promising concept. Graphene’s ability to store and shuttle electrons is an important parameter that might help to circumvent surface diffusion as the rate-limiting step in certain systems. In addition, it should be possible to carry out selective catalytic processes at separate sites. As an example, a preliminary study by Kamat et al. will be quoted.<sup>106</sup> Semiconductor (TiO<sub>2</sub>) and metal nanoparticles (Pt) were embedded in reduced graphene oxide layers to catalyze the water splitting reaction (Figure 6).

The semiconductor nanoparticles, eventually in combination with dyes or CdSe, are supposed to serve as light harvesting sites and induce the oxidation reaction. The electrons are captured by rGO and shuttled across the two-dimensional



**Figure 6.** Combination of a semiconductor photocatalyst (TiO<sub>2</sub>) and metal nanoparticles (Pt) on reduced graphene oxide for the water-splitting reaction.



Scheme 6. Covalent Functionalization of  $sp^2$ -Hybridized Carbons<sup>a</sup>

<sup>a</sup>(a) Diels–Alder reaction, (b) Prato reaction, (c) Diazonium chemistry, (d) alkylation of graphene oxide/activated graphenes, (e) azidation, (f) halogenation, (g) nitrene addition, and (h) Bingel reaction.

scaffold to the platinum nanoparticles, which would facilitate hydrogen reduction. It is known that different  $sp^2$ -hybridized carbons can act as photosensitizer rather than adsorbent or dispersing agent when combined with semiconductor NPs.<sup>107</sup> Such a combination of a photocatalyst ( $\text{TiO}_2$ ) and a “conventional” metal catalyst shows how cooperative catalysis could be established with distinct catalytic moieties. The conductive nature of the support is a prerequisite in this setup and brings new opportunities for the design of next-generation catalysts.

**2.3. Chemically Modified Graphenes.** In addition to rather straightforward chemistry founded on surface-bound oxygen and carbonyl moieties, a plethora of reactions has been established to create diverse functionalities that break ground for the grafting of molecular catalysts on graphenes and related materials. Some of the most important routes are depicted in Scheme 6.

Most  $sp^2$ -hybridized carbon scaffolds (including carbon nanotubes, fullerenes and graphitic carbon shells) are amenable to these reactions; hence, it is not suggestive to discriminate between the different allotropes if it comes to covalent surface chemistry. Several examples will be given for the different reaction types: Diels–Alder reactions are common tools for the derivatization of graphene-like carbons<sup>108</sup> and fullerenes,<sup>109,110</sup> although the reversibility of this reaction limits its applicability to some extent. The rates of cycloaddition and -reversion strongly depend on the electronic properties of the diene and dienophile, respectively; however, most cycloadducts are quite stable at moderate temperatures. The 1,3-dipolar cycloaddition of azomethine ylides to alkenes is one of the most common methods for the construction of nitrogen-containing carbon derivatives. The decarboxylation of iminium salts, resulting

from the condensation of  $\alpha$ -amino acids with aldehydes, is the easiest way to create such ylides. It became the method of choice for the synthesis of substituted fulleropyrrolidines (Prato reaction).<sup>111</sup>

In contrast to Diels–Alder or Bingel cycloadducts, the five-membered ring systems are considered very stable, albeit Retro–Prato reactions can occur under certain conditions.<sup>112</sup> Another reaction that was reported to yield nitrogen-containing heterocyclic derivatives of graphenes involves the decomposition of azide precursors (e.g., perfluorophenyl azides<sup>113</sup>) to form nitrene compounds and, ultimately, aziridines. The decomposition of diazonium salts was initially developed for the functionalization of graphitic surfaces with aryl radicals,<sup>114,115</sup> but proved to be applicable to a broad range of carbons. Halogenation reactions alone, such as iodination via a modified Hunsdiecker reaction<sup>116</sup> or fluorination,<sup>117</sup> usually do not provide a significant advantage for the grafting of molecular catalysts; however, halogenated graphenes are susceptible to alkylation reactions (e.g., via  $\text{RX}$  in  $\text{Li}/\text{NH}_3(\text{l})$ )<sup>118</sup> that normally proceed only via oxidized forms of graphite and graphene.

Another interesting case is the azide modification of graphitic surfaces with iodine azide.<sup>119,120</sup> This account on covalent chemistry taking place on aromatic carbon allotropes is by no means comprehensive, but it will highlight the versatility of the different reactions and the potential for anchoring molecular catalysts. Although in principle applicable to every aromatic carbon surface, the highest degree of diversity was realized on carbon nanotubes.

### 3. CARBON NANOTUBES

In 1976, Oberlin and Endo were the first to report carbon fibers in various shapes around a hollow tube along the fiber axis (2–



50 nm diameter).<sup>121</sup> Stacks of carbon layers were oriented parallel to the fiber axis and arranged in concentric sheets. However, it eventually took a high-impact publication in 1991 to enable another boost for carbon nanotube (CNT) research.<sup>122</sup> CNTs are almost exclusively composed of  $sp^2$ -bonding carbon atoms and can be categorized in two forms: single- and multiwalled carbon nanotubes (SWNTs and MWNTs). SWNTs are semiconductors that behave like quantum wires (1D system) in which the electrons are confined along the tube axis. Two main factors govern the electronic properties: the tube diameter and its helicity (armchair, zigzag, or chiral). MWNTs show graphite-like conductivity at high temperatures and 2D-quantum features at low temperatures.<sup>123</sup> In the case of MWNTs, the distances between adjacent layers are close to the interlayer distance in graphite. Most synthetic protocols involve the formation of other carbon allotropes (amorphous carbon and fullerenes) and sometimes (i.e., in vapor phase synthesis), large bundles (ropes) of several dozen CNTs are yielded rather than single nanotubes. Removal of the metal catalyst during purification is another severe issue. A number of intrinsic properties make CNTs attractive for catalytic applications, for example, graphite-like walls and sufficient surface area. Organized carbon nanomaterials such as CNTs are more stable toward oxidation (about 650 °C) than activated carbon but more reactive than graphite.<sup>124</sup> A lot of properties resemble graphene, such as the possibility of tuning the hydrophobicity via grafting of functional groups or intercalation of metals into the interstices.<sup>125</sup> In addition, the presence of a hollow channel gives rise to new physical properties (confinement effect).

**3.1. Carbocatalysis.** Carbon nanotubes, especially slightly oxygenated forms, are efficient catalysts for oxidative dehydrogenations. In the catalytic hydrogenation of ethylbenzene to styrene, a process of high industrial relevance, CNTs performed better than activated carbon and graphite as catalysts.<sup>126</sup> It was reasoned that the aromatics were first adsorbed on the surface via  $\pi$ -interactions next to basic oxygen moieties, which facilitated dehydrogenation with concomitant formation of surface hydroxy groups.<sup>127</sup> The catalytic activity of MWNTs could be also explained with a (weak) curvature effect, since exfoliated carbons performed less efficiently. Another example, which will be quoted in lieu of many others, is the oxidative dehydrogenation of *n*-butane to 1-butene.<sup>128</sup>

**3.2. Metal Nanoparticles on Carbon Nanotubes.** Several methods (e.g., ion exchange, organometallic grafting, incipient wetness impregnation, electron beam evaporation) are commonly used to prepare metal nanoparticle/CNT composites.<sup>129</sup> Pristine CNTs do usually not possess a high density of functional groups on the surface; hence, surface defects are the predominant anchoring sites for metals. Upon chemical (acids, oxidants) or thermal treatment, the number of oxygen bearing functional groups (as well as the surface area) and, therefore, the loading with metal nanoparticles is increased. In addition, the possibility of filling the nanotubes<sup>130</sup> (Figure 7, right) or intercalation of metals in the intertubular layers, especially in SWNT bundles, has been reported.<sup>131</sup> Nevertheless, the degree of surface functionalization is the most intriguing difference between activated carbon, graphite and CNTs when it comes to the immobilization of metal NPs.<sup>133</sup>

An interesting approach to controlling the dispersion of nanoparticles on CNTs involves the covalent modification of the surface with a monolayer of 4-aminobenzene via electrochemical reduction of nitrobenzene diazonium salt.<sup>134</sup> Grafting

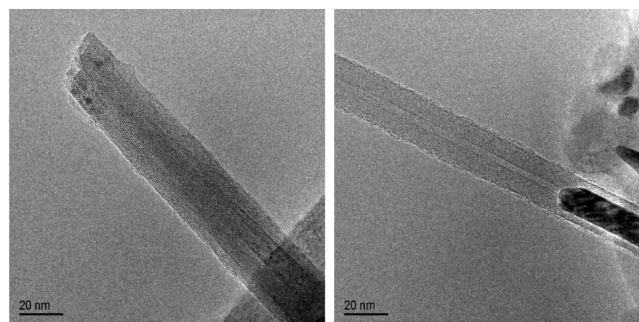
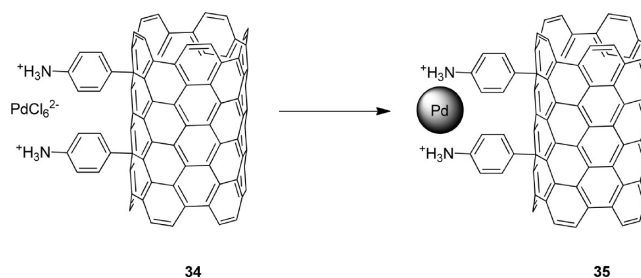


**Figure 7.** Transmission electron microscopy images of hollow (left) and iron-filled (right) carbon nanotubes prepared by solid-state microwave arcing<sup>132</sup> (recorded by Dr. F. Krumeich, ETH Zurich).

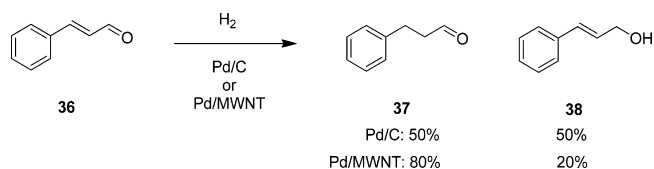
of the aryl moieties and reduction of the nitro groups to the corresponding amines is carried out in one step. Palladium salt is then adsorbed onto the amine moieties via electrostatic interactions, and nanoparticle decorated CNTs **35** are produced via potentiostatic reduction (Scheme 7).

**Scheme 7. CNTs Covalently Functionalized with a 4-Aminobenzene Monolayer and Decorated with Pd Nanoparticles**

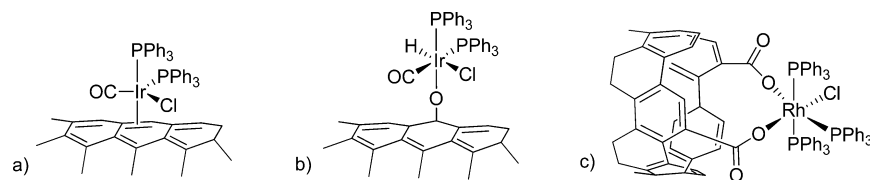


The most prominent application for metal nanoparticle decorated CNTs is hydrogenation catalysis. Notably, the regioselectivities observed can be quite different from those obtained with other carbon-supported catalysts. An interesting example is the hydrogenation of cinnamaldehyde **36** (Scheme 8). MWNTs with Pd-NPs exclusively decorated on the interior

**Scheme 8. Regioselectivity in the Hydrogenation of Cinnamaldehyde **36** with Pd/C and Pd/MWNT, Respectively**



of the nanotubes showed a remarkable selectivity.<sup>135</sup> Whereas Pd/C resulted in arbitrarily distributed reduction products (i.e., hydrocinnamaldehyde **37** and phenyl propanol **38**), Pd/MWNT yielded aldehyde **37** as the major (80%) product at comparable reaction rates. Notably, the formation of cinnamyl alcohol was never observed. The authors reasoned that the lack of oxygenated surface groups at the inner walls of the MWCNTs might explain these results, but also, many other differences (e.g., the lack of micropores) might account for the rendered regioselectivity.

Scheme 9. Coordination Modes of Different Complexes on CNTs<sup>a</sup>

<sup>a</sup>(a)  $\eta^2$  coordinate of  $[\text{IrCl}(\text{CO})(\text{PPh}_3)_2]$  on pristine SWNTs. (b) Hydroxyl-coordinated Ir(III) complex on  $\text{KMnO}_4$ -oxidized SWNTs. (c) Wilkinson's catalyst coordinated to terminal carboxy groups on  $\text{HNO}_3$ -oxidized MWNTs.

In addition to supported palladium, Ru/MWNT, Pt/MWNT (surface area  $\approx 25 \text{ m}^2 \text{ g}^{-1}$ ) and Pt/graphite (surface area  $\approx 300 \text{ m}^2 \text{ g}^{-1}$ ) were used to catalyze the self-same reaction. Ru/MWNT achieved somewhat higher selectivity in aldehyde hydrogenation than Pt/graphite.<sup>136</sup> Other catalytically relevant metal/nanotube composites consist of gold and ruthenium alloys.<sup>137,138</sup> Zhang et al. found that Co/CNTs are highly active and selective formylation catalysts for 1-octene.<sup>139</sup> Konya and co-workers suggested that the activity and selectivity of MWNTs decorated with metallic nanoparticles can depend on their preparation. Indeed, studies concerning CO hydrogenation over Co and Fe catalysts indicated a correlation between activity and reducibility of the metal precursor.<sup>140</sup> When metal acetates were used as precursors rather than metal oxide nanoparticles, the activity of the final MWNT supported metal catalyst was higher and showed altered selectivity. This was attributed to unreactive “oxide spots”, probably residues of the metal oxide nanoparticles used. This is by far not the only example in which the fraction of metal, metal oxide, but also the metal carbide, is essential for the catalytic performance.

**3.2.1. Confinement Effects Inside CNTs.** The efficiency of Fischer–Tropsch iron catalysts supported on CNTs is one of the most intriguing examples for confinement effects inside carbon nanotubes. In addition, in situ XRD investigations proved that the multistep phase transformation of  $\text{Fe}_2\text{O}_3$  to FeO and, ultimately, iron (carbide) occurs at a much lower temperature at each reduction step when the magnetite particles are located inside nanotubes, which may also be tagged as the “confinement effect”.<sup>141</sup> Moreover, the reaction intermediates may be trapped within the nanotubes, which would mean prolonged contact time with the metal particles and, therefore, increased chain growth. Indeed, the yield of  $\text{C}_{5+}$  hydrocarbons was twice as high as with Fe/CNTs catalysts that exposed their catalytic centers predominantly on the outer surface. A study by Dalai et al. might suggest an additional increase in the lifetime of the catalytic system because sintering of the discrete nanoparticles is hampered by the spatial restrictions within the nanochannels.<sup>142</sup> Whether the activity of the Fe-*in*-CNTs is increased, as well, probably because of a more reduced iron state with a higher tendency toward iron carbides, remains unclear at the moment.<sup>141,142</sup> Nevertheless, the recurrence of iron carbide (FeC,  $\text{Fe}_3\text{C}$ ) species is believed to be crucial for high activity in the Fischer–Tropsch synthesis.<sup>141</sup> The aforementioned lack of oxygenated surface groups at the inner surface of CNTs might contribute to this effect.

The confinement effect is more pronounced when CNTs with smaller channel diameters are applied.<sup>143</sup> Naturally, the mean size of the metal clusters is affected by the nanotube diameter and the potentially higher activity of smaller nanoparticles might contribute to all previously mentioned phenomena. The effects of confinement inside CNTs are not

restricted to iron catalysts for Fischer–Tropsch synthesis, of course. The altered performance of metal nanoparticles and molecular catalysts on the interior and exterior of carbon nanotubes is an inspiring approach and has already been the subject of excellent reviews.<sup>144</sup>

**3.2.2. Macronization of CNTs.** In addition to the scale-up of carbon nanotube synthesis, several strategies for their “macronization”<sup>145</sup> have been developed. This strategy should enable efficient catalyst/product separation from liquid-phase reactions (which can be challenging for nanoscopic matter; see section 5) while maintaining a high surface area. For instance, the vertical growth of aligned SWNTs on a macroscopic surface was established by the direct decomposition of gaseous hydrocarbons over a Co/Mo catalyst.<sup>146–148</sup> Nevertheless, aligned CNTs have been employed mainly in the field of electronics or filtration technologies, whereas examples for catalytic applications remain scarce. Janowska et al. reported on a dense and homogeneous layer of aligned Pd-doped MWNTs, which were attached on the inner wall of a silica reactor. The MWNT/ $\text{SiO}_2$  tube was directly used as mechanical stirrer for the hydrogenation of cinnamaldehyde **36** to hydrocinnamaldehyde **37** (90% selectivity, 80% yield).<sup>145</sup> Aligned MWNTs were also grown directly inside the Si channels of a microreactor by thermal chemical vapor deposition (CVD) of ferrocene in xylene.<sup>149</sup> A 20 nm-thick aluminum layer was required to ensure irreversible attachment of the nanotubes prior to impregnation of the carbon nanotubes with a Pt salt solution. The hydrosilylation of 1-octene (1.15 M in toluene) with dimethylphenylsilane (0.96 M) was chosen as a model reaction (flow rate:  $1 \mu\text{L min}^{-1}$ ,  $50 \text{ }^\circ\text{C}$ ) and demonstrated the increased lifetime of the catalyst system due to decreased metal leaching. A three-dimensional array of vertically aligned carbon nanofilaments was synthesized by CVD on  $\text{TiO}_x$  substrates and applied in the oxygen reduction reaction (ORR, see section 2.2.1) after Pt deposition.<sup>150</sup> “Bucky paper” (BP) is an especially interesting representative of a macroscopic material consisting of vertically aligned CNTs, since it combines high mechanical strength and flexibility.  $\text{Fe}_2\text{O}_3$ -NPs supported on BP was employed as a catalyst for the desulfurization of  $\text{H}_2\text{S}$  in a classical fixed-bed configuration.<sup>151</sup> Despite the comparatively low abundance of catalytic applications for “macronized” nanomatter, this concept could boost the feasibility of nanoscopic catalysts in industry.

**3.3. Molecular Catalysts on Carbon Nanotubes.** Just as the case in the immobilization of metal nanoparticles on CNTs, the degree of surface oxidation is of utmost importance for the grafting of molecular catalysts. Pristine nanotubes form only (weak)<sup>152</sup>  $\eta^2$  coordinates with metal complexes such as  $[\text{IrCl}(\text{CO})(\text{PPh}_3)_2]$ , which are of limited catalytic value. Pretreated (i.e.,  $\text{KMnO}_4$ -oxidized) SWNTs formed a hexacoordinated Ir(III) complex after oxidative addition to surface-bound hydroxyl moieties (Scheme 9).<sup>153</sup>

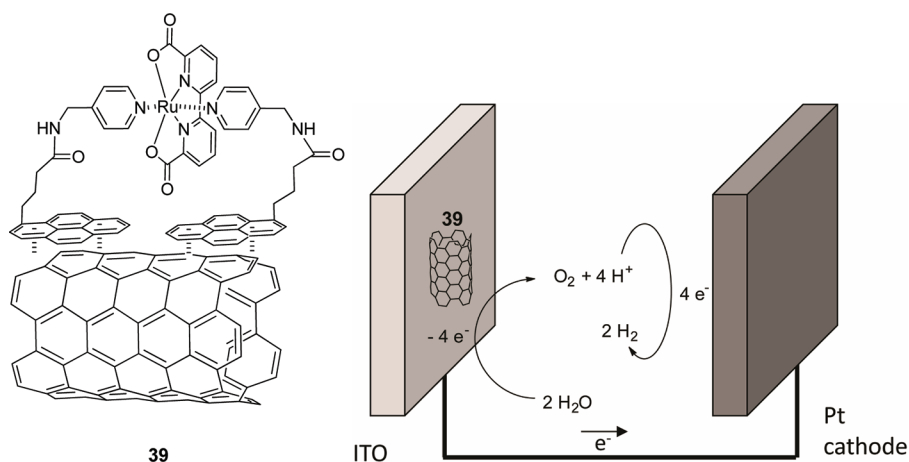


**Figure 8.** MWNT-immobilized Ru(bpa)(pic)<sub>2</sub>-based catalyst 39 for the water-splitting reaction (left); electrochemical cell for water-splitting (right).

As previously mentioned (section 2.1), the oxidation of sp<sup>2</sup>-hybridized carbons creates mainly alcohols within the plain and predominantly carboxylic acids at the edges and defects. Hence, a different coordination mode was proposed for the impregnation of nitric acid-treated MWNTs with [HRh(CO)-(PPh<sub>3</sub>)<sub>3</sub>].<sup>154</sup> The surface-bound carboxyl groups can be subjected to very simple manipulations to alleviate the formation of organometallic compounds on the nanotubes. Giordano et al. treated them with sodium carbonate to facilitate the coordination of [RhCl(CO)<sub>2</sub>]<sub>2</sub>,<sup>155</sup> whereas Koningsberger and co-workers treated carboxylated nanofibers with thionylchloride and reacted them with anthranilic acid as a ligand for rhodium.<sup>156</sup> Although the oxidation route is undoubtedly the most common and straightforward method to anchor molecular catalysts on nanotubes and carbon fibers, it is basically a degradation process that increases the number of defect sites or even creates detached amorphous fragments after severe treatments. It is surprising that the rich chemistry for covalent functionalization of CNTs<sup>157</sup> had comparatively little impact on the development of catalytic systems, although rather mild conditions can be found among them (see section 2.3).

Another very elegant approach for aqueous catalytic systems involves the noncovalent immobilization of complexes via  $\pi$ -stacking interactions. The benefits are obvious: Pristine nanotubes can be used without any pretreatment or functionalization, and the grafting succeeds simply by mixing catalyst and support in water. The predetermination to water as the solvent is the most incisive limitation, albeit polar organic solvents might be applicable in some cases.<sup>158</sup> This restriction is sometimes negligible; for example, when the catalyst will be applied in the water splitting reaction (Figure 8).<sup>159</sup> A pyrene-tagged Ru(bpa)(pic)<sub>2</sub> (2,2'-bipyridine-6,6-dicarboxylic acid, H<sub>2</sub>bpa; 4-picoline, pic) was anchored on MWNTs, and the nanotube/molecular catalyst assembly 39, electrophoretically deposited on an indium tin oxide glass electrode. Immobilized 39 is currently the most efficient molecular catalyst for the electrocatalytic oxidation of water.

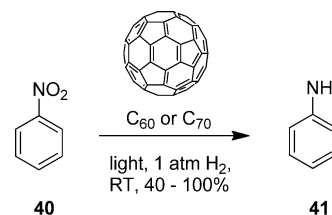
#### 4. FULLERENES

In 1985, the Buckminster fullerenes,<sup>160</sup> molecular allotropes of carbon, were discovered in the gas phase,<sup>161</sup> and their large-scale accessibility by arc vaporization of graphite was disclosed shortly thereafter in 1990.<sup>162</sup> The presence of a closed shell distinguishes fullerenes, which may be considered individual

polyhedral molecules, from all other carbon modifications. Its prominent *I<sub>h</sub>* symmetric C<sub>60</sub> structure contains two distinct C–C bond types: shorter bonds, which define the sides of hexagons, and longer bonds, which are formed between hexagons and pentagons. Because of its nonplanar surface, all conjugated double bonds are strained. Solid C<sub>60</sub> has a rather low specific surface area (10–20 m<sup>2</sup> g<sup>-1</sup>) and sublimates at 707 K.<sup>163</sup> The most reactive bonds in C<sub>60</sub> and C<sub>70</sub> are part of two six-membered rings, which participate, for example, in the formation of transition metal complexes in an  $\eta^2$  fashion.

**4.1. Carbocatalysis.** The most abundant material in heterogeneous catalysis with C<sub>60</sub> is fullerene black (FB), a finely dispersed carbon material extracted from fullerene-containing soot. This label is quite misleading, since FB consists mainly of amorphous carbon and graphitic structures. Further extraction cycles yield different fractions of fullerenes: namely, toluene-soluble (low molecular weight) and quinoline-soluble (higher) fullerenes. However, in contrast to activated charcoal, glassy carbon and graphite, fullerene black is an efficient catalyst for dehydrogenation, cracking, methylation, and demethylation reactions.<sup>164</sup> Photoinduced electron transfer (PET) plays an important role in reduction and oxidation of fullerenes. C<sub>60</sub> and C<sub>70</sub> were found to be suitable catalysts for the reduction of nitrobenzene, using hydrogen gas under UV light (Scheme 10).<sup>165</sup>

#### Scheme 10. C<sub>60</sub> or C<sub>70</sub> and Light-Catalyzed Reduction of Nitrobenzene to Aniline Using H<sub>2</sub> gas (1 atm) As the Terminal Reductant



The same reaction afforded higher gas pressure (4–5 MPa) and temperatures up to 150 °C when carried out in the dark. Improved yields were observed when neutral C<sub>60</sub> was combined with anionic fullerene (C<sub>60</sub><sup>1-</sup>), which was attributed to cooperative electronic effects, albeit it is more likely an effect of residual nickel, as suggested by van Bokhoven et al.<sup>166</sup> C<sub>60</sub><sup>1-</sup>



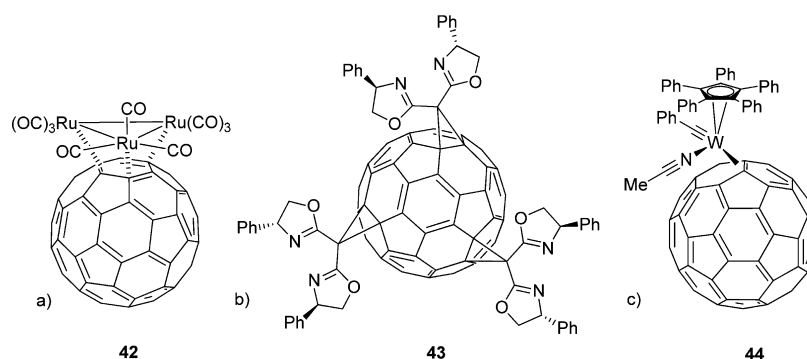


**Figure 9.** Organometallic and purely organic fullerene derivatives: (a)  $C_{60}Ru_3(CO)_9$  complex **42**. (b) Tris adduct of  $C_{60}$  with optically pure methylenebis(oxazoline)s derived from (*R*)-phenylalanine (**43**). (c)  $W(\equiv CPh)(NCMe)(\eta^2-C_{60})(\eta^5-C_5Ph_5)$  complex **44**.

contained nickel up to  $400 \mu\text{g g}^{-1}$  carbon due to the preparation method. Notably, the same compound did not show any catalytic activity when produced via a Ni-free route. It is not self-evident that carbocatalysis is always metal-free, but rather, promoted by transition metal contaminants present at trace levels (down to parts-per-billion or less). Recent publications indicate that this might be a quite abundant problem.<sup>167,168</sup> Because carbon is a natural product, there is potential for contamination by ambient metal sources, or, as described above, by metal-containing reagents during preparation. More important than the origin of a contaminant is, of course, the verification of its absence with the appropriate analytical tools (e.g., atomic absorption spectroscopy, inductively coupled plasma mass spectrometry). This appears vital for any kind of catalytic reaction.

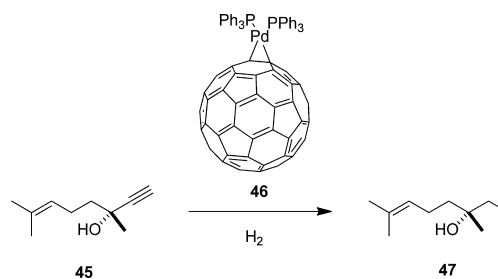
**4.2. Fullerenes As Ligands for Homogeneous Catalysts.** The synthesis of  $C_{60}$  in gram quantities has also raised the interest in the organometallic chemistry of  $C_{60}$  as a ligand. Despite initial reports that claimed  $C_{60}$  to be a highly aromatic molecule, it proved rather unwilling to form stable hexahapto ( $\eta^6-C_{60}$ )M compounds. This has been attributed to its curvature, pointing the exohedral  $\pi$ - $\pi$  orbital away from the perpendicular to the face of the six-membered rings. It was reasoned that  $C_{60}$  is an even weaker ligand toward a single metal than benzene;<sup>169</sup> however, metal triangles provide an effective overlap with the  $\pi$ - $\pi$  orbitals. For example, hexahapto  $C_{60}$  complexes were created with triruthenium,<sup>169</sup> and osmium clusters,<sup>170</sup> respectively.  $C_{60}Ru_3(CO)_9$  complexes (**42**, Figure 9a) can be reduced under mild conditions to form a material that resembles an “organometallic polymer”,<sup>171</sup> a fullerene network linked by low-dimensional Ru clusters, which catalyzed the hydrogenation of cyclohexen-2-one to cyclohexanone.<sup>172</sup> Similar polymeric compounds, so-called metal fullerides ( $C_{60}M_n$ ) consisting of either palladium or platinum, are effective hydrogenation catalysts, e.g., for alkynes, olefins and nitrobenzenes.<sup>173–175</sup>

It is quite interesting that the most active palladium fullerides,  $C_{60}Pd_n$ , are those with  $n > 3$ , whereas for the most active platinum fullerides, a ratio of  $n < 3$  is characteristic. This different behavior might be associated with the localization of the metals in the fullerene frameworks. Pd atoms interacting with more than one  $C_{60}$  seem to be devoid of catalytic activity in hydrogenation reactions. Hence, some Pd acts as only as “glue” in the network, whereas other Pd atoms form the catalytic centers. No such divisions seem to be formed in the case of platinum. Nevertheless, the performance of  $C_{60}Pd_4$  is higher than that of a Pd/C benchmark catalyst.<sup>176</sup>

Under harsh conditions, metal fullerides undergo structural changes, such as fullerene reduction and metal clustering, that result in partial catalyst inactivation (e.g., at temperatures  $>250$  °C for  $C_{60}Pt$ ). The reactivity of fullerenes often resembles moderately electronegative alkenes, as demonstrated by the synthesis of metal-containing<sup>177</sup> and purely organic derivatives (Figure 8). They readily form adducts with radicals, several nucleophiles, and carbenes and participate as a dienophile in a variety of thermal and photochemical cycloaddition reactions. Excellent reviews focus on the vast covalent chemistry of  $C_{60}$ , which is depicted in Scheme 6 to some extent.<sup>178,179</sup> An interesting example of such a covalently functionalized fullerene scaffold is compound **43**, a tris adduct of  $C_{60}$  with optically pure methylenebis(oxazoline) (Figure 9b).<sup>180</sup> The oxazoline moieties are formed between malonate-terminated Bingel fullerenes and (*R*)-phenylalanine to result in  $C_{60}$  derivative **43**, carrying three chiral bis(oxazoline) ligands. Many single metal coordinates of fullerenes have been recently reported in the literature (e.g.,  $W(\equiv CPh)(NCMe)(\eta^2-C_{60})(\eta^5-C_5Ph_5)$  **44**).<sup>181</sup> In general, investigating the reactivity of fullerene-bound organometallics has become an attractive research topic,<sup>182,183</sup> but applications within catalysis remain scarce.

$(\eta^2-C_{60})RhH(CO)(PPh_3)_2$  was used as a catalyst for olefin hydroformylation. It proved to be less efficient than  $RhH(CO)(PPh_3)_2$  but increased the thermal stability of the complex.<sup>184</sup> A similar palladium-based phosphine complex,  $(\eta^2-C_{60})Pd(PPh_3)_2$ , was used for the hydrogenation of the triple bond in 3,7-dimethyl-octa-6-ene-1-in-3-ol (**45**), an important stage in the industrial production of fragrances and vitamins A and E (Scheme 11). Synthesis of compound **46** proceeded straightforward by stirring  $Pd(PPh_3)_4$  at ambient temperature in the presence of Buckminster fullerene. Its activity in hydrogenation reactions was 1 order of magnitude

**Scheme 11.**  $(\eta^2-C_{60})Pd(PPh_3)_2$ -Catalyzed Hydrogenation of 3,7-Dimethyl-octa-6-ene-1-in-3-ol (**45**)





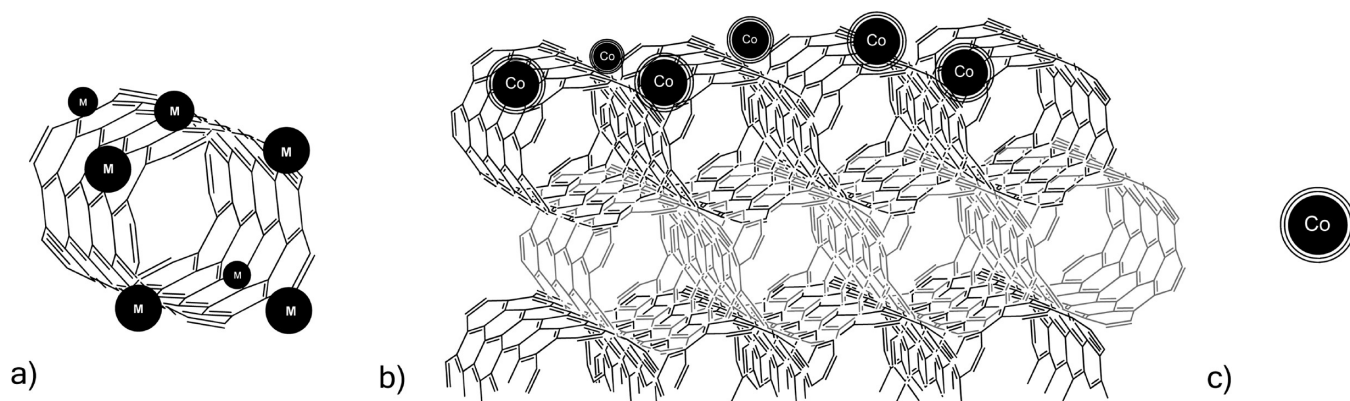
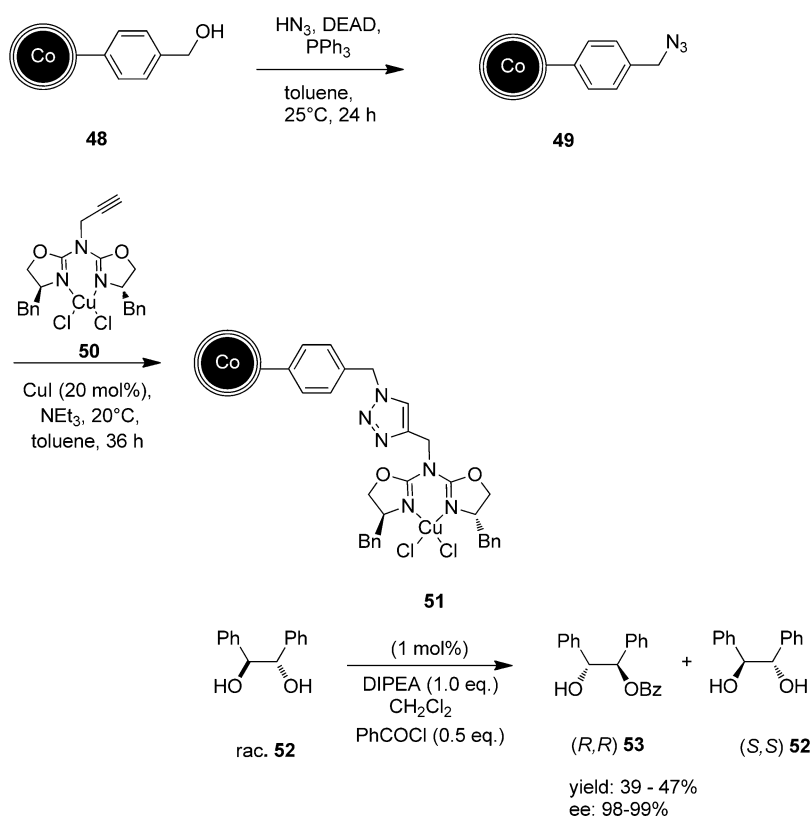


**Figure 10.** Different “magnetic carbons”: (a) magnetite NP-decorated CNT, (b) Co/C-NP decorated OMC, and (c) Co/C-NP.

**Scheme 12. Immobilization of a Chiral Azabis(oxazoline)–Copper Complex (50) on Co/C-NPs via a Diazonium Chemistry/“Click” Approach and Its Application in the Kinetic Resolution of Racemic Diol 52 via Asymmetric Monobenzoylation**



higher compared with a conventional system ( $\text{Pd}/\gamma\text{-Al}_2\text{O}_3$ ), and remarkable selectivity (99.5%) was achieved.<sup>185</sup>

Fullerene-containing Pt complexes are effective promoters in the hydrosilylation of alkenes by triethoxysilane as well.<sup>186</sup> As a consequence of their cage-like structure,  $\text{C}_{60}$  and higher fullerenes can also incarcerate metal atoms. Smalley et al. were the first who prepared a stable endohedral fullerene ( $\text{La}@C_{82}$ ).<sup>187</sup> Theoretical and experimental studies on such compounds related to their electrochemical properties, preparation, and separation can be found in specialized reviews.<sup>188</sup> Briefly, they are both stronger electron donors and acceptors than their fullerene parents. From a practical point of view, endohedral metallofullerenes alone seem less attractive for catalytic applications because of their limited stability under ambient conditions and separation issues.

## 5. SOLVING SEPARATION ISSUES: “MAGNETIC” CARBON

On one hand, the nanoscopic dimensions of novel carbon supports significantly increase the reactant’s accessibility due to the high surface area, whereas the high diffusion rate of the products reduces many side reactions. On the other hand, the small dimensions render quantitative recovery almost impossible by conventional means, which can lead to the blocking of filters and valves. This calls for improved separation modes or even new approaches for the efficient recycling of the heterogeneous catalysts. Albeit certain materials such as carbon nanotubes are amenable to “macronization” (section 3.2.2), this cannot be considered a general method for all carbonaceous materials. One alternative to filtration can be magnetic separation.

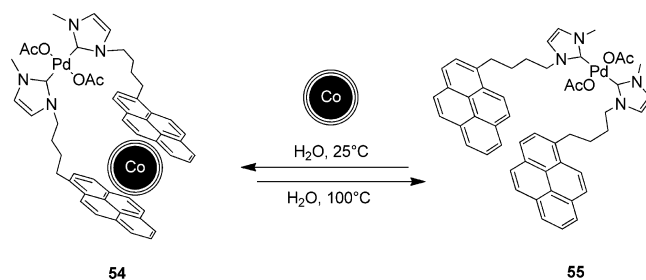
In general, there are two methods to render carbon “magnetic” with different ferromagnetic and superparamagnetic metal (oxide) nanoparticles, respectively. The first way demands decoration of the carbon scaffold’s surface with nanoparticles, which results in materials morphologically similar to the heterogeneous catalysts discussed in the previous sections (Figure 10). Thermal treatment (600 °C) of an activated carbon impregnated with a nickel salt, which results in magnetic Ni-NPs within a carbon matrix, can be considered an example for this approach.<sup>189</sup> Reduced graphene oxide<sup>190</sup> and CNTs<sup>191</sup> were modified with magnetite NPs using well-established methods (Figure 10a). Because of the limited stability of surface exposed nanoparticles, these composites are inherently less stable than the second group of “magnetic” carbons consisting of nanomagnets enclosed in carbon cages.

An elegant study by Schueth et al. might mark the turning point (i.e., progress from metal-decorated carbons toward carbon coated metals), since it combines features of both routes: mesostructured silica was used as a template to synthesize a carbon/silica composite on which cobalt nanoparticles were deposited on the exterior. The Co-NPs were subsequently protected with a nanometer-thick carbon layer before the silica scaffold was removed by aqueous hydrofluoric acid. The pores of the resulting ordered mesoporous carbon (OMC), decorated with Co/C-NPs (Figure 10b), could be impregnated with catalytically active noble metals.<sup>192</sup> Several other groups have reported on iron-filled MWNTs, which were usually prepared by electric arc discharge<sup>193</sup> or chemical vapor deposition,<sup>194</sup> but applications in catalysis remained scarce. Whether CNTs decorated exclusively on the interior with magnetic nanoparticles<sup>195</sup> should be classified as members of the first or second group will be left to the reader. Discrete carbon-coated metal nanoparticles were accessible, as well, for example, via the Huffman–Kraetschmer carbon arc process, CVD, or pyrolysis of metal complexes;<sup>196–198</sup> however, their production has been limited to small-scale operations. Grass et al.<sup>199–201</sup> reported on carbon-coated metal nanoparticles that were produced through reducing flame-spray pyrolysis.<sup>202</sup> This procedure gave rise to substantial amounts of metal nanoparticles (>30 g/h) which is a prerequisite for applications as a catalyst support. Moreover, the thermal and chemical stability of this material, even under harsh acidic conditions, was remarkable.<sup>203–205</sup> Furthermore, the graphene-like layers could be covalently functionalized via diazonium chemistry.<sup>182,206,207</sup>

Stark and Reiser anchored the stable nitroxyl radical 2,2,6,6-tetramethylpiperidine-1-oxyl (TEMPO), an organocatalyst for the chemoselective oxidation of primary and secondary alcohols, on carbon-coated cobalt nanoparticles via a “click” protocol.<sup>208</sup> A chiral azabis(oxazoline)–copper complex (**50**) for the kinetic resolution of racemic 1,2-diol **52** via asymmetric monobenzylation was immobilized in a similar fashion (Scheme 12).<sup>209</sup>

In addition, palladium–PPh<sub>3</sub> complexes for Suzuki–Miyaura cross-coupling reactions were grafted onto carbon-coated cobalt nanoparticles.<sup>210,211</sup> A Pd-NHC (N-heterocyclic carbene) complex (**55**) was tagged with pyrene moieties and contacted with Co/C-NPs in water, thus forming a non-covalently attached catalyst for the aqueous hydroxycarbonylation of arylhalides (Scheme 13). The attraction to the graphitic surface via  $\pi$ -stacking interactions is sufficiently strong to prevent unintended dissociation of the immobilized compound at ambient temperature, thus offering a very concise route for the grafting of catalysts. Desorption of the aromatic

### Scheme 13. A Palladium(NHC) Complex (**55**) Noncovalently Attached to Co/C-NPs via Pyrene Anchors for a Thermally Triggered Catch–Release System



anchors can be thermally triggered to allow the catalyst to become homogeneous during the course of the reaction at 100 °C. Once the reaction is finished and the solution is cooled to ambient temperature, the pyrene moieties bind to the carbon surface, and the absorbed complex **54** is amenable to magnetic decantation. Recycling was demonstrated 16 times, and catalyst leaching into the product phase proved to be negligible.

## 6. CONCLUSIONS

Carbon is maybe the most versatile matrix for catalytic reactions. Some allotropes can be used for applications that call only for a “dirt-cheap” carrier for nanocrystals or a microporous reservoir for metal species (e.g., activated carbons). Already in such “simple” systems, which merely demand a dispersing agent for the catalytic sites, the unique metal–support interactions (adsorption, desorption, readorption) of different carbonaceous materials have a huge impact on the performance of the immobilized species.

The influence of carbon supports on the immobilized catalysts cannot be seen as a consequence of a single physical or chemical property. Whereas high surface areas in excess of 1000 m<sup>2</sup> g<sup>−1</sup> might suggest the use of microporous carbons, such as carbon molecular sieves, in some catalytic applications, other systems require completely different properties. For example, electrode materials for electrocatalysts demand high attrition resistance (boron-doped diamond) and electron conductivity (graphite, graphene). The latter might be the most intriguing discrimination criteria between different carbon allotropes (amorphous carbon vs graphite). Parameters such as the degree of surface functionalization render the conductivity (graphene vs graphene oxide) and influence the loading and dispersion of catalytic sites, respectively. In fact, surface functionalization (e.g., via oxidation) is one of the most important factors to tune the adsorption behavior of carbonaceous surfaces. Naturally, not all adsorption sites are equally amenable to oxygenation. Especially micropores or confined areas (hollow spheres and nanotubes) are less affected, which has interesting implications on the activity or regioselectivity of catalysts located in these sites.

In some cases, a high degree of surface-bound oxygenated moieties is a prerequisite for high activity for various reasons (e.g., increased hydrophilicity or redox activity, Lewis acid type interactions with substrates or catalysts). A rather simple explanation is, of course, that they enable an anchoring point for metal(oxide) NPs or molecular catalysts, but that is not true in every case. In fact, polar surface moieties can also hamper the grafting of catalysts, e.g., molecular catalysts that rely on  $\pi$ -interactions with an aromatic surface. Other catalytic mechanisms involve such interactions between aromatic areas

in the support and substrates, which are inhibited when the surface is functionalized.

Finally,  $\eta^2$  metal complexes can be formed rather than analogs that result from oxidative addition if surface-bound hydroxyl moieties are present. In addition to oxidations, many reactions are known to increase molecular diversity on  $sp^2$ -hybridized carbons, but relatively few have been already implemented in the immobilization of catalysts. It is surprising that the rather harsh and unselective oxidation of carbon surfaces is still the method of choice when it comes to the grafting of transition metal complexes, especially because the presence of oxygenated moieties affects the catalytic performance of the material.

In this field, degradation-free processing of carbonaceous materials might not yet have experienced the attention it certainly deserves. In this regard, perspectives might arise from changing the electronic structure of the support itself: for example in graphene-like scaffolds, via covalent grafting of compounds that feature electron-donating or withdrawing groups. The most elaborate protocols focus on diazonium grafting; nevertheless, applications in catalysis are not yet disclosed.<sup>212</sup> A concept that has been realized to some extent is based on magnetic force to facilitate the often tedious separation (e.g., via centrifugation) of nanoscaled carbon allotropes, either by decoration with or incorporation of magnetic nanoparticles in carbon scaffolds. Such measures that improve the handling of carbons might also strengthen the acceptance of more “complex” chemistry on novel carbon nanomaterials.

## AUTHOR INFORMATION

### Corresponding Author

\*E-mail: wstark@ethz.ch.

### Notes

The authors declare no competing financial interest.

## REFERENCES

- (1) Cowland, F. C.; Lewis, J. C. *J. Mater. Sci.* **1967**, *2*, 507.
- (2) Robertson, J.; O'Reilly, E. P. *Phys. Rev. B* **1987**, *35*, 2946.
- (3) IUPAC, *Compendium of Chemical Terminology*; Blackwell Scientific: Oxford, 1997.
- (4) Dreyer, D. R.; Jia, H.-P.; Bielawski, C. W. *Angew. Chem., Int. Ed.* **2010**, *49*, 6813.
- (5) Dreyer, D. R.; Bielawski, C. W. *Chem. Sci.* **2011**, *2*, 1233.
- (6) Jia, H.-P.; Dreyer, D. R.; Bielawski, C. W. *Tetrahedron* **2011**, *67*, 4431.
- (7) Papirer, E.; Brendle, E.; Ozil, F.; Balard, H. *Carbon* **1999**, *37*, 1265.
- (8) Auer, E.; Freund, A.; Pietsch, J.; Tacke, T. *Appl. Catal., A* **1998**, *173*, 259.
- (9) Rodriguez-Reinoso, F. *Carbon* **1998**, *36*, 159.
- (10) Peigney, A.; Laurent, C.; Flahaut, E.; Bacsá, R. R.; Rousset, A. *Carbon* **2001**, *39*, 507.
- (11) Kutzelnigg, A. *Ber. Dtsch. Chem. Ges. B* **1930**, *63*, 1753.
- (12) Kolthoff, I. M. *J. Am. Chem. Soc.* **1932**, *54*, 4473.
- (13) Rideal, E. K.; Wright, W. M. *J. Chem. Soc. Trans.* **1925**, *127*, 1347.
- (14) Rideal, E. K.; Wright, W. M. *J. Chem. Soc.* **1926**, *129*, 1813.
- (15) Rideal, E. K.; Wright, W. M. *J. Chem. Soc.* **1926**, *129*, 3182.
- (16) Davis, B. H. *J. Catal.* **1983**, *79*, 58.
- (17) Fu, J.; Shi, F.; Thompson, L. T.; Lu, X.; Savage, P. E. *ACS Catal.* **2011**, *1*, 227.
- (18) Fu, J.; Lu, X.; Savage, P. E. *Energy Environ. Sci.* **2010**, *3*, 311.
- (19) Toebe, M. L.; van Dillen, J. A.; de Jong, K. P. *J. Mol. Catal. A: Chem.* **2001**, *173*, 75.
- (20) Sajiki, H.; Hirota, K. *J. Synth. Org. Chem. Jpn.* **2001**, *59*, 109.
- (21) Sajiki, H.; Kume, A.; Hattori, K.; Hirota, K. *Tetrahedron Lett.* **2002**, *43*, 7247.
- (22) Sajiki, H.; Ikawa, T.; Hattori, K.; Hirota, K. *Chem. Commun.* **2003**, 1106.
- (23) Sajiki, H.; Hirota, K. *Chem. Pharm. Bull.* **2003**, *51*, 320.
- (24) Sajiki, H.; Ikawa, T.; Hattori, K.; Hirota, K. *Chem. Commun.* **2003**, 654.
- (25) Ikawa, T.; Sajiki, H.; Hirota, K. *Tetrahedron* **2004**, *60*, 6189.
- (26) Cameron, D. S.; Cooper, S. J.; Dodgson, I. L.; Harrison, B.; Jenkins, J. W. *Catal. Today* **1990**, *7*, 113.
- (27) McNair, R. *J. Chem. Ind.* **1995**, *62*, 1.
- (28) Yin, L.; Liebscher, J. *Chem. Rev.* **2007**, *107*, 133.
- (29) Seki, M. *Synthesis* **2006**, *18*, 2975.
- (30) Novák, Z.; Szabó, A.; Répási, J.; Kotschy, A. *J. Org. Chem.* **2003**, *68*, 3327.
- (31) Koehler, K.; Heidenreich, R. G.; Krauter, J. G. E.; Pietsch, J. *Chem.—Eur. J.* **2002**, *8*, 622.
- (32) Yin, L.; Erdmann, F.; Liebscher, J. *J. Heterocycl. Chem.* **2005**, *42*, 1369.
- (33) LeBlond, C. R.; Andrews, A. T.; Sun, Y.; Sowa, J. R. *Org. Lett.* **2001**, *3*, 1555.
- (34) Zim, D.; Monteiro, A. L.; Dupont, J. *Tetrahedron Lett.* **2000**, *41*, 8199.
- (35) Horiuti, I.; Polanyi, M. *Trans. Faraday Soc.* **1934**, *30*, 1164.
- (36) Augustine, R. L.; Yaghmaie, F.; Van Peppen, J. F. *J. Org. Chem.* **1984**, *49*, 1865.
- (37) Ehwald, H.; Shestov, A. A.; Muzykantov, V. S. *Catal. Lett.* **1994**, *25*, 149.
- (38) Ertl, G. *Chem. Rec.* **2001**, *1*, 33.
- (39) Zaera, F. *Acc. Chem. Res.* **2002**, *35*, 129.
- (40) Augustine, R. L.; O'Leary, S. T. *J. Mol. Catal. A: Chem.* **1995**, *95*, 277.
- (41) Zhao, F.; Bhanage, B. M.; Shirai, M.; Arai, M. *Chem.—Eur. J.* **2000**, *6*, 843.
- (42) Schmidt, A. F.; Mametova, L. V. *Kinet. Catal.* **1996**, *37*, 431.
- (43) Barreto-Rosa, M. M.; Bonnet, M. C.; Tkatchenko, I. *Stud. Surf. Sci. Catal.* **1991**, *59*, 263.
- (44) Bergbreiter, D. E.; Chen, B. *J. Chem. Soc. Chem. Commun.* **1983**, 1238.
- (45) Jayasree, S.; Seayad, A.; Chaudhari, R. V. *J. Chem. Soc., Chem. Commun.* **1999**, 1067.
- (46) Biffis, A.; Zecca, M.; Basato, M. *Eur. J. Inorg. Chem.* **2001**, 1131.
- (47) Lipshutz, B. H.; Tasler, S.; Chrisman, W.; Spliethoff, B.; Tesche, B. *J. Org. Chem.* **2003**, *68*, 1177.
- (48) Rebek, J. *Tetrahedron* **1979**, *35*, 723.
- (49) Bergbreiter, D. E.; Chen, B.; Weatherford, D. *J. Mol. Catal.* **1992**, *74*, 409.
- (50) Davies, I. W.; Matty, L.; Hughes, D. L.; Reider, P. J. *J. Am. Chem. Soc.* **2001**, *123*, 10139.
- (51) Whitesides, G. M.; Hackett, M.; Brainard, R. L.; Lavalleye, J. P. P. M.; Sowinski, A. F.; Izumi, A. N.; Moore, S. S.; Brown, D. W.; Staudt, E. M. *Organometallics* **1985**, *4*, 1819.
- (52) Widegren, J. A.; Bennett, M. A.; Finke, R. G. *J. Am. Chem. Soc.* **2003**, *125*, 10301.
- (53) Widegren, J. A.; Finke, R. G. *J. Mol. Catal. A: Chem.* **2003**, *198*, 317.
- (54) Park, K. H.; Chung, Y. K. *Adv. Synth. Catal.* **2005**, *347*, 854.
- (55) Volpin, M. E.; Novikov, Y. N.; Lapkina, N. D.; Kasatochkin, V. I.; Struchkov, Y. T.; Kazakov, M. E.; Stukan, R. A.; Povitskij, V. A.; Karimov, Y. S.; Zvarikina, A. V. *J. Am. Chem. Soc.* **1975**, *97*, 3366.
- (56) Such-Basanez, I.; Roman-Martinez, M. C.; Salinas-Martinez de Lecea, C. *Carbon* **2004**, *42*, 1357.
- (57) Pyun, J. *Angew. Chem., Int. Ed.* **2011**, *50*, 46.
- (58) Mermin, N. D. *Phys. Rev.* **1968**, *176*, 250.
- (59) Novoselov, K. S.; Geim, A. K.; Morozov, S. V.; Jiang, D.; Zhang, Y.; Dubonos, S. V.; Grigorieva, I. V.; Firsov, A. A. *Science* **2004**, *306*, 666.



- (60) Zacharia, R.; Ulbricht, H.; Hertel, T. *Phys. Rev. B: Condens. Matter Mater. Phys.* **2004**, *69*, 155406.
- (61) Katsnelson, M. I. *Mater. Today* **2007**, *10*, 20.
- (62) Morozov, S. V.; Novoselov, K. S.; Geim, A. K. *Phys.-Usp.* **2008**, *51*, 744.
- (63) Castro Neto, A. H.; Guinea, F.; Peres, N. M. R.; Novoselov, K. S.; Geim, A. K. *Rev. Mod. Phys.* **2009**, *81*, 109.
- (64) Katsnelson, M. I.; Novoselov, K. S. *Solid State Commun.* **2007**, *143*, 3.
- (65) Falko, V. I.; Kechedzhi, K.; McCann, E.; Altshuler, B. L.; Suzuura, H.; Ando, T. *Solid State Commun.* **2007**, *143*, 33.
- (66) Chen, D.; Tang, L.; Li, J. *Chem. Soc. Rev.* **2010**, *39*, 3157.
- (67) Burghard, M.; Klauk, H.; Kern, K. *Adv. Mater.* **2009**, *21*, 2586.
- (68) Berger, C.; Song, Z. M.; Li, X. B.; Wu, X. S.; Brown, N.; Naud, C.; Mayou, D.; Li, T. B.; Hass, J.; Marchenkov, A. N.; Conrad, E. H.; First, P. N.; de Heer, W. A. *Science* **2006**, *312*, 1191.
- (69) Sutter, P. W.; Flege, J. I.; Sutter, E. A. *Nat. Mater.* **2008**, *7*, 406.
- (70) Park, S.; Ruoff, R. S. *Nat. Nanotechnol.* **2009**, *4*, 217.
- (71) Coleman, J. N. *Adv. Funct. Mater.* **2009**, *19*, 3680.
- (72) Ismach, A.; Druzgalski, C.; Penwell, S.; Schwartzberg, A.; Zheng, M.; Javey, A.; Bokor, J.; Zhang, Y. *Nano Lett.* **2010**, *10*, 1542.
- (73) Suzuki, Y.; Matsushima, M.; Kodomari, M. *Chem. Lett.* **1998**, 319.
- (74) Sereda, G. A.; Rajpara, V. B.; Slaba, R. L. *Tetrahedron* **2007**, *63*, 8351.
- (75) Klemens, P. G.; Pedraza, D. F. *Carbon* **1994**, *32*, 735.
- (76) Garrigues, B.; Laporte, C.; Laurent, R.; Laporterie, A.; Dubac, J. *Liebigs Ann.* **1996**, 739.
- (77) Garrigues, B.; Laurent, R.; Laporte, C.; Laporterie, A.; Dubac, J. *Liebigs Ann.* **1996**, 743.
- (78) Han, B. H.; Shin, D. H.; Cho, S. Y. *Tetrahedron Lett.* **1985**, *26*, 6233.
- (79) Dreyer, D. R.; Park, S.; Bielawski, C. W.; Ruoff, R. S. *Chem. Soc. Rev.* **2010**, *39*, 228. 1.
- (80) Lee, S. H.; Dreyer, D. R.; An, J.; Velamakanni, A.; Piner, R. D.; Park, S.; Zhu, Y.; Kim, S. O.; Bielawski, C. W.; Ruoff, R. S. *Macromol. Rapid Commun.* **2010**, *31*, 281.
- (81) Hummers, W. S.; Offeman, R. E. *J. Am. Chem. Soc.* **1958**, *80*, 1339.
- (82) Buchsteiner, A.; Lerf, A.; Pieper, J. *J. Phys. Chem. B* **2006**, *110*, 22328.
- (83) Cervený, S.; Barroso-Bujans, F.; Alegria, A.; Colmenero, J. *J. Phys. Chem. C* **2010**, *114*, 2604.
- (84) Lerf, A.; He, H.; Forster, M.; Klinowski, J. *J. Phys. Chem. B* **1998**, *102*, 4477.
- (85) He, H.; Riedl, T.; Lerf, A.; Klinowski, J. *J. Phys. Chem.* **1996**, *100*, 19954.
- (86) Lerf, A.; He, H.; Riedl, T.; Forster, M.; Klinowski, J. *Solid State Ionics* **1997**, 101.
- (87) Szabo, T.; Berkesi, O.; Forgo, P.; Josepovits, K.; Sanakis, Y.; Petridis, D.; Dekany, I. *Chem. Mater.* **2006**, *18*, 2740.
- (88) Jia, H.-P.; Dreyer, D. R.; Bielawski, C. W. *Adv. Synth. Catal.* **2011**, *53*, 528.
- (89) Scheuermann, G. M.; Rumi, L.; Steurer, R.; Bannwarth, W.; Muelhaupt, R. *J. Am. Chem. Soc.* **2009**, *131*, 8262.
- (90) Stankovich, S.; Dikin, D. A.; Dommett, G. H. B.; Kohlhaas, K. M.; Zimney, E. J.; Stach, E. A.; Piner, R. D.; Nguyen, S. T.; Ruoff, R. S. *Nature* **2006**, *442*, 282.
- (91) Siamaki, A. R.; El Rahman, A.; Khder, S.; Abdelsayed, V.; El-Shall, M. S.; Gupton, B. F. *J. Catal.* **2011**, *279*, 1.
- (92) Moussa, S.; Siamaki, A. R.; Gupton, B. F.; El-Shall, M. S. *ACS Catal.* **2012**, *2*, 145.
- (93) Lu, G.-Q.; Wieckowski, A. *Curr. Opin. Colloid Interface Sci.* **2000**, *5*, 95.
- (94) Shang, N. G.; Papakonstantinou, P.; McMullan, M.; Chu, M.; Stamboulis, A.; Potenza, A.; Dhessi, S. S.; Marchetto, H. *Adv. Funct. Mater.* **2008**, *18*, 3506.
- (95) Griese, S.; Kampouris, D. K.; Kadara, R. O.; Banks, C. E. *Electroanal.* **2008**, *20*, 1507.
- (96) Ji, X.; Kadara, R. O.; Krussma, J.; Chen, Q.; Banks, C. E. *Electroanal.* **2010**, *22*, 7.
- (97) Sine, G.; Duo, I.; El Roustom, B.; Foti, G.; Comninellis, C. J. *Appl. Electrochem.* **2006**, *36*, 847.
- (98) Ikeda, T.; Boero, M.; Huang, S.-F.; Terakura, K.; Oshima, M.; Ozaki, J.-I. *J. Phys. Chem. C* **2008**, *112*, 14706.
- (99) Shao, Y.; Sui, J.; Yin, G.; Gao, Y. *Appl. Catal. B: Environ.* **2008**, *79*, 89.
- (100) Sidik, R. A.; Anderson, A. B.; Subramanian, N. P.; Kumaraguru, S. P.; Popov, B. N. *J. Phys. Chem. B* **2006**, *110*, 1787.
- (101) Seger, B.; Kamat, P. V. *J. Phys. Chem. C* **2009**, *113*, 7990.
- (102) Ogasawara, T.; Debart, A.; Holzapfel, M.; Novak, P.; Bruce, P. G. *J. Am. Chem. Soc.* **2006**, *128*, 1390.
- (103) Debart, A.; Paterson, A. J.; Bao, J.; Bruce, P. G. *Angew. Chem., Int. Ed.* **2008**, *47*, 4521.
- (104) Lu, Y.-C.; Xu, Z.; Gasteiger, H. A.; Chen, S.; Hamad-Schifferli, K.; Shao-Horn, Y. *J. Am. Chem. Soc.* **2010**, *132*, 12170.
- (105) McCloskey, B. D. K.; Scheffler, R.; Speidel, A.; Bethune, D. S.; Shelby, R. M.; Luntz, A. C. *J. Am. Chem. Soc.* **2011**, *133*, 18038.
- (106) Kamat, P. V. *J. Phys. Chem. Lett.* **2010**, *1*, 520.
- (107) Wang, W. D.; Serp, P.; Kalck, P.; Silva, C. G.; Faria, J. L. *Mater. Res. Bull.* **2008**, *43*, 958.
- (108) Sarkar, S.; Bekyarova, E.; Niyogi, S.; Haddon, R. C. *J. Am. Chem. Soc.* **2011**, *133*, 3324.
- (109) Hudhomme, P. C. R. *Chim.* **2006**, *9*, 881.
- (110) Wilson, S. R.; Wu, Y. *Chem. Commun.* **1993**, 78.
- (111) Prato, M.; Maggini, M. *Acc. Chem. Res.* **1998**, *31*, 519.
- (112) Martín, N.; Altable, M.; Filippone, S.; Martín-Domenech, A.; Echegoyen, L.; Cardona, C. M. *Angew. Chem., Int. Ed.* **2006**, *45*, 110.
- (113) Liu, L.-H.; Lerner, M. M.; Yan, M. *Nano Lett.* **2010**, *10*, 3754.
- (114) Allongue, P.; Delamar, M.; Desbat, B.; Fagebaume, O.; Hitmi, R.; Pinson, J.; Saveant, J.-M. *J. Am. Chem. Soc.* **1997**, *119*, 201.
- (115) Bourdillon, C. *J. Electroanal. Chem.* **1992**, 336, 113.
- (116) Coleman, K. S.; Chakraborty, A. K.; Bailey, S. R.; Sloan, J.; Alexander, M. *Chem. Mater.* **2007**, *19*, 1076.
- (117) Lee, Y.-S. *J. Fluorine Chem.* **2007**, *128*, 392.
- (118) Chakraborty, S.; Guo, W.; Hauge, R. H.; Billups, W. E. *Chem. Mater.* **2008**, *20*, 3134.
- (119) Hassner, A. *Acc. Chem. Res.* **1971**, *4*, 9.
- (120) Devadoss, A.; Chidsey, C. E. D. *J. Am. Chem. Soc.* **2007**, *129*, 5370.
- (121) Oberlin, A.; Endo, M. *J. Cryst. Growth* **1976**, *32*, 335.
- (122) Iijima, S. *Nature* **1991**, *354*, 56.
- (123) Bethune, D. S.; Kiang, C. H.; Devries, M. S.; Gorman, G.; Savoy, R.; Vazquez, J.; Beyers, R. *Nature* **1993**, *363*, 605.
- (124) Serp, P.; Corrias, M.; Kalck, P. *Appl. Catal., A* **2003**, *253*, 337.
- (125) Terrones, M.; Wen Kuang, H.; Kroto, Y. W.; Walton, D. R. M. *Top. Curr. Chem.* **1999**, *199*, 189.
- (126) Pham-Huu, C.; Keller, N.; Charbonniere, L. J.; Ziessel, R.; Ledoux, M. J. *Chem. Commun.* **2000**, 19, 1871.
- (127) Mestl, G.; Maksimova, N. I.; Keller, N.; Roddatis, V. V.; Schloegl, R. *Angew. Chem., Int. Ed.* **2001**, *113*, 2122.
- (128) Zhang, J.; Liu, X.; Blume, R.; Zhang, A.; Schloegl, R.; Su, D. S. *Science* **2008**, *322*, 73.
- (129) Benoit, L.; Begin, D.; Ledoux, M.-J.; Pham-Huu, C. *Ordered Porous Solids Chapter 23*; pp 621–649.
- (130) Monthieux, M. *Carbon* **2002**, *40*, 1809.
- (131) Govindaraj, A.; Satishkumar, B. C.; Nath, M.; Rao, C. N. R. *Chem. Mater.* **2000**, *12*, 202.
- (132) Liang, Y.-C.; Hwang, K. C.; Lo, S.-C. *Small* **2008**, *4*, 405.
- (133) Zhong, Z.; Liu, B.; Sun, L.; Ding, J.; Lin, J.; Tan, K. L. *Chem. Phys. Lett.* **2002**, *135*, 362.
- (134) Guo, D. J.; Li, H. L. *Electrochem. Commun.* **2004**, *6*, 999.
- (135) Tessonnier, J.-P.; Pesant, L.; Ehret, G.; Ledoux, M. J.; Pham-Huu, C. *Appl. Catal., A* **2005**, *288*, 203.
- (136) Planeix, J. M.; Coustel, N.; Coq, B.; Brotons, V.; Kumbhar, P. S.; Dutartre, R.; Geneste, P.; Bernier, P.; Ajayan, P. M. *J. Am. Chem. Soc.* **1994**, *116*, 7935.



- (137) Han, L.; Wu, W.; Kirk, F. L.; Luo, J.; Maye, M. M.; Kariuki, N. N.; Lin, Y.; Wang, C.; Zhong, C.-J. *Langmuir* **2004**, *20*, 6019.
- (138) Hermans, S.; Sloan, J.; Shephard, D. S.; Johnson, B. F. G.; Green, M. L. H. *Chem. Commun.* **2002**, 276.
- (139) Zhang, H.; Qiu, J.; Liang, C.; Li, Z.; Wang, X.; Wang, Y.; Feng, Z.; Li, C. *Catal. Lett.* **2005**, *101*, 211.
- (140) Gucci, L.; Stefler, G.; Geszti, O.; Koppány, Z.; Kónya, Z.; Molnár, E.; Urbánc, M.; Kiricsi, I. *J. Catal.* **2006**, *244*, 24.
- (141) Chen, W.; Fan, Z.; Pan, X.; Bao, X. *J. Am. Chem. Soc.* **2008**, *130*, 9414.
- (142) Malek Abbaslou, R. M.; Tavassoli, A.; Soltan, J.; Dalai, A. K. *Appl. Catal., A* **2009**, *367*, 47.
- (143) Malek Abbaslou, R. M.; Soltan, J.; Dalai, A. K. *Appl. Catal., A* **2010**, *379*, 129.
- (144) Pan, X.; Bao, X. *Acc. Chem. Res.* **2011**, *44*, 553.
- (145) Janowska, I.; Wine, G.; Ledoux, M.-J.; Pham-Huu, C. *J. Mol. Catal. A: Chem.* **2007**, *267*, 92.
- (146) Hu, M.; Murakami, Y.; Ogura, M.; Maruyama, S.; Okubo, T. *J. Catal.* **2004**, *225*, 230.
- (147) Maruyama, S.; Einarsson, E.; Murakami, Y.; Edamura, T. *Chem. Phys. Lett.* **2005**, *403*, 320.
- (148) Zhang, L.; Tan, Y.; Resasco, D. E. *Chem. Phys. Lett.* **2006**, *422*, 198.
- (149) Ishigami, N.; Ago, H.; Motoyama, Y.; Takasaki, M.; Shinagawa, M.; Takahashi, K.; Ikutac, T.; Tsuji, M. *Chem. Commun.* **2007**, 1626.
- (150) Ruvinskiy, P. S.; Bonnefont, A.; Houille, M.; Pham-Huu, C.; Savinova, E. R. *Electrochim. Acta* **2010**, *55*, 3245.
- (151) Deneuve, A.; Wanga, K.; Janowska, I.; Chizaria, K.; Edouarda, D.; Ersenb, O.; Ledoux, M.-J.; Pham-Huu, C. *Appl. Catal. A: Gen.* **2011**, *400*, 230.
- (152) Banerjee, S.; Wong, S. S. *J. Am. Chem. Soc.* **2002**, *124*, 8940.
- (153) Banerjee, S.; Wong, S. S. *Nano Lett.* **2002**, *2*, 49.
- (154) Zhang, Y.; Zhang, H.-B.; Lin, G.-D.; Chen, P.; Yuan, Y.-Z.; Tsai, K. R. *Appl. Catal., A* **1999**, *187*, 213.
- (155) Giordano, R.; Serp, P.; Kalck, P.; Kihn, Y.; Schreiber, J.; Marhic, C.; Duval, J.-L. *Eur. J. Inorg. Chem.* **2003**, *4*, 610.
- (156) Ros, T. G.; van Dillen, A. J.; Geus, G. W.; Koningsberger, D. C. *Chem.—Eur. J.* **2002**, *8*, 868.
- (157) Karousis, N.; Tagmatarchis, N.; Tasis, D. *Chem. Rev.* **2010**, *110*, 5366.
- (158) Liu, G.; Wu, B.; Zhang, J.; Wang, X.; Shao, M.; Wang, J. *Inorg. Chem.* **2009**, *48*, 2383.
- (159) Li, F.; Zhang, B.; Li, X.; Jiang, Y.; Chen, L.; Li, Y.; Sun, L. *Angew. Chem., Int. Ed.* **2011**, *123*, 12484.
- (160) Kroto, H. W. *Angew. Chem., Int. Ed.* **1992**, *31*, 111.
- (161) Kraetschmer, W.; Lamb, L. D.; Fostiropoulos, K.; Huffman, D. R. *Nature* **1990**, *347*, 354.
- (162) Kroto, H. W.; Heath, J. R.; O'Brien, S. C.; Curl, R. F.; Smalley, R. E. *Nature* **1985**, *318*, 162.
- (163) Coq, B.; Planeix, J. M.; Brotons, V. *Appl. Catal., A* **1998**, *173*, 175.
- (164) Fursikov, P. V.; Kushch, C. D.; Muradyan, V. E.; Davydova, G. I.; Knerelman, E. I.; Moravsky, A. P. *Mol. Mater.* **2000**, *13*, 319.
- (165) Li, B.; Xu, Z. *J. Am. Chem. Soc.* **2009**, *131*, 16380.
- (166) Pacosova, L.; Kartusch, C.; Kukula, P.; van Bokhoven, J. A. *ChemCatChem* **2011**, *3*, 154.
- (167) Buchwald, S. L.; Bolm, C. *Angew. Chem., Int. Ed.* **2009**, *48*, 5586.
- (168) Leadbeater, N. E. *Nat. Chem.* **2010**, *2*, 1007.
- (169) Hsu, H.-F.; Shapley, J. R. *J. Am. Chem. Soc.* **1996**, *118*, 9192.
- (170) Lee, K.; Choi, Z.-H.; Cho, Y.-J.; Song, H.; Park, J. T. *Organometallics* **2001**, *20*, 5570.
- (171) Wohlers, M.; Herzog, B.; Belz, T.; Bauer, A.; Braun, T.; Ruhle, T.; Schlögl, R. *Synth. Met.* **1996**, *77*, 55.
- (172) Braun, T.; Wohlers, M.; Belz, T.; Nowitzke, T.; Wortmann, G.; Ushida, Y.; Pfander, N.; Schlögl, R. *Catal. Lett.* **1997**, *43*, 167.
- (173) Nagashima, H.; Kato, Y.; Yamagushi, H.; Kimura, E.; Kawanishi, T.; Kato, M.; Saito, Y.; Haga, M.; Itoh, K. *Chem. Lett.* **1994**, 1207.
- (174) Nagashima, H.; Nakaoka, A.; Saito, Y.; Kato, M.; Kawanishi, T.; Itoh, K. *J. Chem. Soc., Chem. Comm.* **1992**, 377.
- (175) Nagashima, H.; Nakaoka, A.; Tajima, S.; Saito, Y.; Itoh, K. *Chem. Lett.* **1992**, 1361.
- (176) Goldshleger, N. F. *Fullerene Sci. Technol.* **2001**, *9*, 255.
- (177) Hawkins, J. M.; Meyer, A.; Lewis, T. A.; Loren, S.; Hollander, F. J. *Science* **1991**, *252*, 312.
- (178) Diederich, F.; Thilgen, C. *Science* **1996**, *271*, 317. b.
- (179) Diederich, F.; Gómez-López, M. *Chem. Soc. Rev.* **1999**, *28*, 263.
- (180) Thilgen, C.; Diederich, F. *Chem. Rev.* **2006**, *106*, 5049.
- (181) Yeh, W.-Y. *Angew. Chem., Int. Ed.* **2011**, *123*, 12252 and references cited therein.
- (182) Park, B. K.; Miah, M. A.; Lee, G.; Cho, Y.-J.; Lee, K.; Park, S.; Choi, M.-G.; Park, J. T. *Angew. Chem.* **2004**, *116*, 1744.
- (183) Yeh, W.-Y.; Tsai, K.-Y. *Organometallics* **2010**, *29*, 604.
- (184) Claridge, J. B.; Douthwaite, R. E.; Green, M. L. H. *J. Mol. Catal.* **1994**, *89*, 113.
- (185) Sulman, E.; Matveeva, V.; Semagina, N.; Yanov, I.; Bashilov, V.; Sokolov, V. *J. Mol. Catal. A: Chem.* **1999**, *146*, 257.
- (186) Fang, P. F.; Chen, Y. Y.; Wang, Z. H.; Lu, Q. S. *Chin. J. Org. Chem.* **1999**, *19*, 600.
- (187) Heath, J. R.; O'Brien, S. C.; Zhang, Q.; Liu, Y.; Curl, R. F.; Kroto, H. W.; Tittel, F. K.; Smalley, R. E. *J. Am. Chem. Soc.* **1985**, *107*, 7779.
- (188) Sherigara, B. S.; Kutner, W.; D'Souza, F. *Electroanalysis* **2003**, *15*, 753.
- (189) Gorria, P.; Sevilla, M.; Blanco, J. A.; Fuertes, A. B. *Carbon* **2006**, *44*, 1954.
- (190) Chandra, V.; Park, J.; Chun, Y.; Lee, J. W.; Hwang, I.-C.; Kim, K. S. *ACS Nano* **2010**, *5*, 3979.
- (191) Stoffelbach, F.; Aqil, A.; Jerome, C.; Jerome, R.; Detrembleur, C. *Chem. Commun.* **2005**, 4532.
- (192) Lu, A.-H.; Schmidt, W.; Matoussevitch, N.; Bonnemann, H.; Spliethoff, B.; Tesche, B.; Bill, E.; Kiefer, W.; Schueth, F. *Angew. Chem., Int. Ed.* **2004**, *43*, 4303.
- (193) Saito, Y. *Carbon* **1995**, *33*, 979.
- (194) Muller, C.; Hampel, S.; Elefant, D.; Biedermann, K.; Leonhardt, A.; Ritschel, M.; Buchner, B. *Carbon* **2006**, *44*, 1746.
- (195) Korneva, G.; Ye, H.; Gogotsi, Y.; Halverson, D.; Friedman, G.; Bradley, J.-C.; Kornev, K. G. *Nano Lett.* **2005**, *5*, 879.
- (196) Hayashi, T.; Hirono, S.; Tomita, M.; Umemura, S. *Nature* **1996**, *381*, 772.
- (197) Teunissen, W.; de Groot, F. M. F.; Geus, J.; Stephan, O.; Tence, M.; Colliex, C. *J. Catal.* **2001**, *204*, 169.
- (198) Lu, A.-H.; Li, W.-C.; Matoussevitch, N.; Spliethoff, B.; Bonnemann, H.; Schueth, F. *Chem. Commun.* **2005**, 98.
- (199) Grass, R. N.; Athanassiou, E. K.; Stark, W. J. *Angew. Chem., Int. Ed.* **2007**, *46*, 4909.
- (200) Herrmann, I. K.; Grass, R. N.; Mazunin, D.; Stark, W. J. *Chem. Mater.* **2009**, *21*, 3275.
- (201) Grass, R. N.; Stark, W. J. *J. Mater. Chem.* **2006**, *16*, 1825.
- (202) Stark, W. J.; Madler, L.; Maciejewski, M.; Pratsinis, S. E.; Baiker, A. *Chem. Commun.* **2003**, 588.
- (203) Koehler, F. M.; Rossier, M.; Waelle, M.; Athanassiou, E. K.; Limbach, L. K.; Grass, R. N.; Guenther, D.; Stark, W. J. *Chem. Commun.* **2009**, *32*, 4862.
- (204) Rossier, M.; Koehler, F. M.; Athanassiou, E. K.; Grass, R. N.; Aeschlimann, B.; Guenther, D.; Stark, W. J. *J. Mater. Chem.* **2009**, *19*, 8239.
- (205) Schaetz, A.; Zeltner, M.; Michl, T. D.; Rossier, M.; Fuhrer, R.; Stark, W. J. *Chem.—Eur. J.* **2011**, *17*, 10566.
- (206) Tan, C. G.; Grass, R. N. *Chem. Commun.* **2008**, 4297.
- (207) Fuhrer, R.; Athanassiou, E. K.; Luechinger, N. A.; Stark, W. J. *Small* **2009**, *5*, 383.
- (208) Schaetz, A.; Grass, R. N.; Stark, W. J.; Reiser, O. *Chem.—Eur. J.* **2008**, *14*, 8262.
- (209) Schaetz, A.; Grass, R. N.; Kainz, Q. M.; Stark, W. J.; Reiser, O. *Chem. Mater.* **2010**, *22*, 305.

(210) Zeltner, M.; Schaetz, A.; Hefti, M. L.; Stark, W. J. *J. Mater. Chem.* **2011**, *21*, 2991.

(211) Schaetz, A.; Long, T. R.; Grass, R. N.; Stark, W. J.; Hanson, P. R.; Reiser, O. *Adv. Funct. Mater.* **2010**, *20*, 4323.

(212) Koehler, F. M.; Luechinger, N. A.; Ziegler, D.; Athanassiou, E. K.; Grass, R. N.; Rossi, A.; Hierold, C.; Stemmer, A.; Stark, W. J. *Angew. Chem., Int. Ed.* **2009**, *48*, 224.